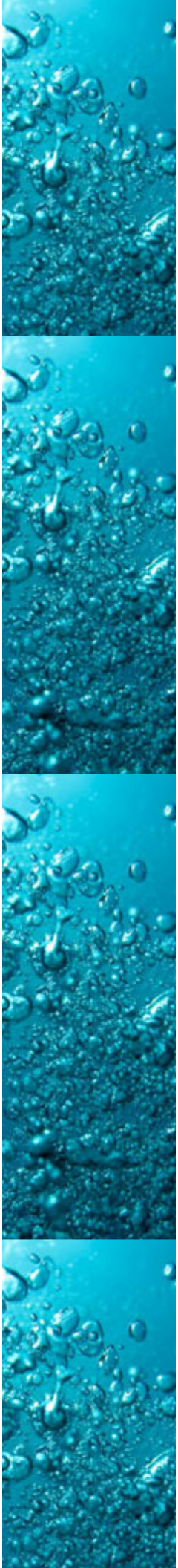

Steering Product Formation in Anaerobic Digestion Systems:

The effect of elevated CO_2 partial pressure on the fermentative degradation of pyruvate and butyrate by a mixed microbial consortium

MSc. Thesis
María Paola Gómez Páez

January 2019

TU Delft Delft University of Technology
Faculty of Civil Engineering and Geosciences

Steering Product Formation in Anaerobic Digestion Systems:

The effect of elevated CO_2 partial pressure on the fermentative degradation of pyruvate and butyrate by a mixed microbial consortium

---

Author: María Paola Gómez Páez

For the degree of: Master of Science in Civil Engineering

To be defended publicly on: Monday January 28, 2019 at 12:00 PM

Faculty of Civil Engineering and Geosciences

Department of Water Management

Section Sanitary Engineering

Graduation committee:

	Delft University of Technology
Prof. dr. ir. J.B. van Lier	Faculty of Civil Engineering and Geosciences Section Sanitary Engineering
Dr. ir. R.E.F. Lindeboom	Faculty of Civil Engineering and Geosciences Section Sanitary Engineering
Dr. R. Kleerebezem	Faculty of Applied Sciences Section Environmental Biotechnology
Ir. Pamela Cerón Chafla	Faculty of Civil Engineering and Geosciences Section Sanitary Engineering

TU Delft Delft University of Technology
Faculty of Civil Engineering and Geosciences

ACKNOWLEDGEMENTS

I would like to express my gratitude to my thesis assessment committee Proffesor Jules van Lier, Assistant Proffesor Robbert Kleerebezem, Assistant Professor Ralph Lindeboom and Ir. Pamela Cerón, for their support, valuable comments and very constructive feedback throughout the development of my MSc thesis project. I highly appreciate them sharing their knowledge and their passion for anaerobic wastewater treatment and biotechnology with such great enthusiasm, as this has truly encouraged me to produce an outcome I'm quite satisfied with.

I warmly thank Ir. Pamela Cerón for her valuable daily support and guidance both at the laboratory and during the development of the analyses and the report. Very special thanks to the laboratory technicians, PhD researchers and MSc students working at the WaterLab, for their help and very friendly disposition.

Finally, I would like to thank my family and friends for their unconditional love and support throughout the development of my MSc studies at TU Delft. I can truly say that I'll be finalizing my MSc studies with a wealth of new knowledge that I'm excited to make the most of during the next steps of my career.

ABSTRACT

In the context of steering product formation in anaerobic digestion systems, the present thesis work elaborates on the potential role of elevated CO_2 partial pressures as an environmental driver that may influence end-product selectivity from methane towards compounds from the carboxylic platform. As an emerging field of research, organic acid production via mixed culture fermentation is currently in an exploratory phase and the understanding of basic functional principles driving each of the biochemical conversions of interest is of vital importance.

The present investigation forms part of a series of studies conjunctively aimed at elucidating the effect of elevated CO_2 partial pressures on glucose fermentation, which consists of a complex network of several metabolic routes. Specifically, this thesis work focuses on the effects of CO_2 partial pressure on the degradation of two key metabolites that are central and/or highly relevant to the glucose conversion pathways, namely pyruvate and butyrate. While butyrate is one of the common metabolites in the fermentative conversion of a range of complex organic compounds –including glucose-, pyruvate is the branching-point of the metabolic pathways in glucose fermentation. In this sense, the degradation of pyruvate may lead to the formation of butyrate and/or a wide range of different intermediate/end-products, as dictated by the prevailing biological, environmental, thermodynamic and kinetic conditions of the anaerobic system under consideration.

For the purpose of evaluating the faith of both pyruvate and butyrate fermentations under different CO_2 conditions, a series of batch experiments at CO_2 partial pressures of 0.2, 1.0, 3.0, 5.0 and 8.0 bar were conducted for each of these substrates. Using a flocculent mixed microbial consortium as the inoculum, pyruvate and butyrate were provided at initial concentrations of approximately 1 g Pyruvate-COD.l^{-1} and 1.1 g Buyrate-COD.l^{-1}. In following the biochemical conversions taking place in each case, the relative concentrations of the main metabolites and final products being consumed and/or formed in each of the experiments were monitored and measured in time. Based on the identification of the concentrations of the predominant compounds present in the reactors, COD balances were constructed in each case.

In further elucidating the effects of elevated CO_2 partial pressures -up to 8.0 bar- on the fermentation of pyruvate and butyrate, the stoichiometries of the main biochemical reactions that were involved in the degradation of these organic acids were derived as part of this study. Based on these balanced stoichiometries, an evaluation of indicative thermodynamic potentials were also derived for the main conversion steps. Indicative analyses of the reaction energetics were subsequently complemented with the

determination of indicative kinetic quantities, including substrate/metabolite consumption and/or production rates for specific metabolites of concern. The outcomes from these thermodynamic and kinetic analyses were essential in understanding the response of pyruvate and butyrate degrading bacteria/archaea to increasing CO_2 levels. In general terms, it was found that the prevailing CO_2 partial pressures in the reactors had a role in promoting or inhibiting specific metabolic routes. In addition to the role of CO_2 as a substrate or a product in carboxylation or decarboxylation reactions, respectively, varying CO_2 partial pressures had an impact on the pH of the liquid broth. Specifically, in the presence of a buffering capacity of 100 mM $NaHCO_3$, pH's in the reactors were estimated at 6.9, 6.6, 6.5, 6.4 and 6.2, corresponding to operation at CO_2 partial pressures of 0.2, 1.0, 3.0, 5.0 and 8.0 bar, respectively.

According to the experimental outcomes, methane was the dominant end product in both the pyruvate and butyrate degradation experiments. Regarding the pyruvate trials, CH_4 accounted for between 35 ± 22% and 68 ± 3.0% of the COD by the end of the 3.0 and 0.2 pCO_2 experiments, while acetate and methane formation followed a downward trend. Thus, higher CO_2 partial pressures in the pyruvate experiments were coincident with enhanced formation of alternative metabolites, predominantly propionate. According to the experimental data, propionate formation yields increased from 0.24 ± 0.01 mg Propionate-COD.mg^{-1} Pyruvate-COD up to 0.34 ± 0.01 Propionate-COD.mg^{-1} Pyruvate-COD during the 0.2 and 8.0 bar pCO_2 experiments, respectively. In contrast, the results from the butyrate experiments indicate that methane production tended to increase in response to elevated pCO_2's, with the fraction of CH_4-COD increasing from 42 ± 1.7% to 74 ± 19% when operating at 0.2 and 3.0 bar pCO_2, respectively. While CH_4 formation by hydrogenotrophic archaea was promoted at increasing pCO_2's, with the occurrence of a lag phase, the degradation of butyrate via either acetate or propionate formation was negatively impacted by elevated pCO_2's. Thus, in line with the findings for both the pyruvate and butyrate experiments, it was found that while elevated pCO_2's promoted formation of products that are a result of carboxylation reactions, it correlated with a decrease in the formation of products that are a result of a decarboxylation step.

Following identification of the main product spectrums, indicative ΔG values were estimated for the main biochemical conversions in the pyruvate and butyrate metabolic networks. In absence of precise information on the actual concentrations for all relevant intermediate metabolites, including succinate, these thermodynamic calculations were based on a concentration of 1mM, as a physiologically plausible concentration for this intermediate metabolite, as reported in the literature [63, 64]. Similarly, with H_2 partial pressures remaining below the equipment's detection limit of 60 Pa for all experiments, energy yield calculations were based on H_2 partial pressures of 1 and 60 Pa, which correspond to the average pH_2 expected in properly functioning anaerobic digesters [15] and the equipment's detection limit, respectively.

With indicative ΔG values ranging between approximately -105 kJ/mol and -88 kJ/mol at all pCO_2 conditions tested and pH_2's of between 1 and 60 Pa, the conversion of pyruvate into acetate was the most thermodynamically favorable reaction in the pyruvate fermentation experiments. The energetic viability of this conversion did however decrease in response to increasing CO_2 partial pressures. Although all other reactions were exergonic at the conditions of these experiments, their energy yields were lower with indicative ΔG values ranging between -60 kJ/mol and -10 kJ/mol. In agreement with the propensity for more propionate formation at increasing pCO_2's, the indicative thermodynamic favorability of the conversion of pyruvate to propionate at an indicative pH_2 of 60 Pa evidenced an increase from -50 kJ/mol to -60 kJ/mol for the experiments conducted at 0.2 and 8.0 bar pCO_2, respectively. While the oxidation of butyrate into acetate was the most thermodynamically favorable reaction at all the pCO_2's conditions tested during the butyrate fermentation experiments (i.e. indicative Gibbs free energy changes ranging between -61 kJ/mol and -36 kJ/mol at pCO_2's of between 0.2 and 8.0 bar and H_2 partial pressures of between 1 and 60 Pa), the energy yields from the conversion of butyrate into acetate also followed a downward trend with increasing pCO_2's.This trend for decreased acetate formation from butyrate was a consequence of high CO_2 partial pressures leading to a corresponding decrease in the operating pH's, from a pH of 6.9 for the 0.2 pCO_2 experiments down to a pH of 6.2 during the 8.0 bar batch tests. Similarly, the indicative energy yields associated with the degradation of butyrate into propionate appeared less negative in response to elevated CO_2 partial pressures, with indicative energy yields decreasing from -52 kJ/mol to -45 kJ/mol and from -21 kJ/mol to -13 kJ/mol between 0.2 and 8.0 bar pCO_2's at the assumed boundary H_2 partial pressures of 1 Pa and 60 Pa, respectively. This trend for lower energy yields at increasing pCO_2's was a result of the conversion of butyrate to propionate corresponding to a decarboxylation step.

Estimates of the apparent degradation rates for pyruvate indicated that increasingly high CO_2 partial pressures correlated with a decrease in the rates of pyruvate conversion. In particular, while the consumption rate for pyruvate was estimated at approximately 435 mg Pyruvate.l^{-1}.d^{-1} when operating at a pCO_2 of 0.2 bar, the indicative degradation rate of this substrate was determined as approximately 181 mg Pyruvate.l^{-1}.d^{-1} for the 8.0 bar pCO_2 trials, corresponding to a reduction in this rate of approximately 58%. Regarding the indicative degradation rates for butyrate, increasingly high CO_2 partial pressures correlated with an apparent reduction in the conversion rates for this substrate, with rates decreasing from 86 mg Butyrate.l^{-1}.d^{-1} at a pCO_2 of 0.2 bar down to approximately 15 mg Butyrate.l^{-1}.d^{-1} when operating at 8.0 bar pCO_2, which corresponded to a decline in this conversion rate in excess of 80%. Thus, it appears that elevated CO_2 availability in the systems may have led to a certain extent of inhibition of the activity of (-potentially) rate limiting enzymes catalyzing pyruvate and/or butyrate degradation. With no formal measurements of enzymatic activities, this hypothesis was however not confirmed as part of this study.

CONTENTS

LIST OF FIGURES

LIST OF TABLES

1. INTRODUCTION

1.1. Background and problem description

Fundamental and applied research in (waste-) water treatment lays at the core of innovative and successful technological developments that can path the way towards the achievement of the circular economy goals [49, 50]. One such technological development, the well-known anaerobic digestion process, although widely and successfully applied in the treatment of a range of industrial and municipal (waste-) waters, is a biotechnological process well worth exploring further [42, 43].

While current anaerobic digestion applications are effective units for energy recovery via complete mineralization of organic compounds into methane, an increasing interest exists in evaluating the potential of anaerobic processes for the recovery of alternative, higher added-value compounds, in the form of e.g. short chain carboxylates/organic acids [22, 50].

In the context of steering product formation in anaerobic digestion systems, the prospects of mixed culture fermentation for the production of chemical building-blocks from a range of organic feedstocks are promising, and significant efforts have been directed towards research at a proof of principle level [24]. While the outcomes from these studies have provided very valuable insight into the great potential of this technology, the need for a detailed evaluation of the biochemical mechanisms and environmental conditions that govern value-added product accumulation is to be further explored [17, 52, 53].

In this sense, achieving an adequate understanding of the mechanistic implications of certain environmental parameters, of which pH, temperature, salinity and/or composition of the headspace may be significant in increasing the selectivity of undefined mixed culture fermentations, is a key pre-requisite in optimizing organic acid accumulation and recovery from anaerobic digestion [22, 24].

As observed by several authors [24, 22, 59], one parameter with a potential influence on steering product formation in fermentative degradation applications corresponds to the prevailing CO_2 partial pressures in the headspace of anaerobic configurations. In particular, one direct implication of the addition of CO_2 that may contribute to a shift in the product spectrum in fermentative degradation systems corresponds to its effect on the liquid's phase pH. Of relevance for the present investigation, as per the calculations presented in Section 3.3., in the presence of a buffering capacity of 100mM $NaHCO_3$, increasingly high CO_2 partial pressures of 0.2, 1.0, 3.0, 5.0 and 8.0 bar led to a

corresponding acidification of the fermentative broth, with pH values estimated at 6.9, 6.6, 6.5, 6.4 and 6.2, respectively.

In view of the potentially interesting effects that elevated CO_2 partial pressures may have as a mechanisms that can be used to influence product selectivity in fermentative applications, the present thesis work seeks to contribute to the body of knowledge on this specific topic, through an investigation of the effects of elevated CO_2 partial pressures on the fermentative degradation of two specific organic acids, namely pyruvate and butyrate. In the context of evaluating the impact of pCO_2 as a potential driver in the fermentation of e.g. glucose, pyruvate and butyrate were chosen as the substrates of concern considering that the microorganisms that are involved in either pyruvate and/or butyrate fermentation are expected to react differently to varying pCO_2 levels in the system. In particular, while pyruvate is a focal metabolite which degradation routes directly involve carboxylation and/or decarboxylation steps (i.e. consumption and/or release of CO_2 in the formation of either propionate and/or acetate, respectively) [60, 61], butyrate is an intermediate compound which main degradation route does not directly involve consumption and/or release of CO_2 (i.e. oxidation of butyrate into 2 moles of acetate) [16, 62].

In *contributing* towards the elucidation of the effects of varying CO_2 partial pressures on the fermentative degradation of pyruvate and butyrate, the research and analysis that was conducted as part of this thesis work was guided by the research questions and hypothesis that have been formulated in Section 1.2 below.

1.2. Research Questions

The main objectives of the present investigation can be delineated via the following three main research questions:

1. Will the selectivity of key end/intermediate metabolites in pyruvate and butyrate fermentation change in response to elevated CO_2 partial pressures?

Hypothesis: operating at increasingly higher CO_2 partial pressures may lead to a shift in the product spectrum of pyruvate degradation towards preferential formation of metabolites that result from carboxylation reactions (e.g. propionate). On the other hand, considering that CO_2 is neither consumed nor produced in the fermentative degradation of butyrate into e.g. acetate, it is expected that the product spectrum associated to butyrate fermentation will remain relatively unchanged at all pCO_2's conditions tested.

2. Can operating at elevated pCO_2's up to 8.0 bar have an effect on the energetic viability of specific metabolic pathways involved in the anaerobic degradation of pyruvate and butyrate?

Hypothesis: while increasing CO_2 partial pressures will lead to a decreased thermodynamic viability of pyruvate decarboxylation reactions, the change of Gibbs free energy associated to pyruvate conversions that involve a carboxylation step will become more negative. Regarding the energetic viability of butyrate conversion, it is hypothesized that no substantial change will be observed due to varying pCO_2 conditions.

3. Are the specific degradation and/or conversion rates of pyruvate, butyrate and/or their associated intermediate metabolites affected by operation at elevated CO_2 partial pressures?

Hypothesis: it is expected that the conversion rates of pyruvate, butyrate and associated intermediate metabolites can potentially be negatively impacted by elevated CO_2 partial pressures, as this operating variable could have an inhibitory effect on the metabolic activities of the microorganisms involved in the degradation of these compounds.

1.3. Research Approach and Thesis Lay-out

As a first step to undertaking the present research work, a targeted literature review was conducted that allowed an understanding of the fundamental principles of anaerobic degradation of organic compounds, with particular emphasis on the implications of operating these systems at elevated pCO_2's. Additionally, current information on the use of fermentative technologies towards targeted production of organic acids, as well as detailed research reporting on the degradation routes of pyruvate and butyrate have also been reviewed and considered. In this sense, Chapter 2 provides a summary of the key theoretical concepts that are relevant to identifying the impacts of elevated CO_2 partial pressures on pyruvate and butyrate fermentation, in terms of its *indicative* effect on the product spectrum, thermodynamic and kinetic viability of the main metabolic routes involved in the degradation of these compounds, as per the scope of this investigation.

Chapter 3 provides an overview of the materials and analytical methods that were used in conducting the laboratory scale batch experiments carried out as part of this research work, including the experimental set-up, analytical techniques, as well as the most relevant details on the design and operation of the batch reactor configurations.

Based on the analysis of the experimental data, the product spectrums associated with the anaerobic degradation of pyruvate and butyrate at initial pCO_2's of 0.2, 1.0. 3.0, 5.0 and 8.0 bar (i.e. equilibrium pCO2's of approximately 0.2, 1.0, 1.5, 2.0 and 3.5, respectively), are presented in Section 4.1 of Chapter 4. Once the product spectrums were derived, the main metabolic routes that lead to the formation of these products in pyruvate and butyrate fermentation are presented in Section 4.2.

Sections 4.3 and 4.4 provide an overview of the outcomes of a high-level assessment of the *indicative* effect that elevated pCO_2's may have on the energetic and kinetic viabilities of the main anaerobic conversions taking place in pyruvate and butyrate fermentations, respectively.

Following the results and discussion presented in Chapter 4, Chapter 5 provides key concluding remarks highlighting the most relevant findings on the use of CO_2 as a potential mechanisms to influence product formation in pyruvate and butyrate fermentation processes, as evaluated in this investigation.

2. THEORETICAL BACKGROUND

2.1. Anaerobic degradation of complex organic compounds

Anaerobic degradation of organic matter to CO_2 and CH_4, the most oxidized and reduced forms of carbon, respectively, is a multi-step process where intermediate metabolites constitute the input for subsequent biochemical conversions [15].

This multi-step conversion is the result of the interaction of different physiological types of bacteria and archaea, namely fermentative, acetogenic and methanogenic microorganisms. Such synthrophic microbial consortia are thus able to effectively mineralize complex organic compounds in a process initiated by the hydrolysis and fermentation of these compounds into H_2, CO_2, formate, acetate and reduced organic compounds, including propionate, butyrate, lactate, succinate and ethanol. These reduced compounds can also be subsequently oxidized to acetate, H_2 and CO_2 by acetogenic bacteria. As a last step, methanogenic archaea utilize acetate, H_2 plus carbonate, formate or methanol to produce CH_4, CO_2 and new cell material [16].

Within this metabolic network, acetogenic bacteria are heavily reliant on synthrophic mechanisms that ensure biochemical conversion of short-chain fatty acids (e.g. butyrate and propionate) into acetate, CO_2, formate and hydrogen is energetically favorable [17, 30, 31, 32].

The importance of acetogenesis and the corresponding occurrence of synthrophic interactions in the complete mineralization of organic compounds is further made evident when considering that approximately 76% of the energy flow that is involved in methane production from complex organic sources proceeds via the oxidation of reduced organic intermediates [18, 19, 20, 21]. An overview of the relative distribution of the energy flow in the mineralization of complex organic matter towards methane formation is provided in Figure 2-1.

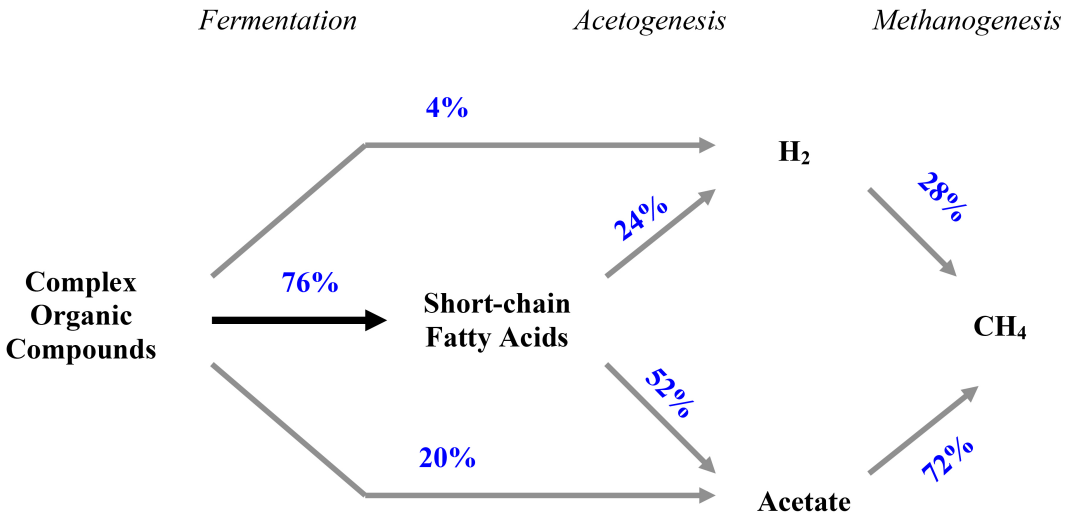

Figure 2-1. Methanogenic mineralization of complex organic matter and the distribution of the energy content involved in complex matter to methane formation
(Adapted from: McCarty, 1982)

In anaerobic environments however, methanogenic archaea maintain low H_2, formate and acetate concentrations, which in turn make e.g. propionate and butyrate degradation feasible [22, 29].

2.1.1. Relevance of pyruvate as a central metabolite in fermentation processes

Pyruvate, an organic compound containing a carboxylic acid group (R-COOH) and a ketone group (RC(=O)R', with R and R' being carbon-containing substituents), is an alpha-keto (α-keto) acid with a significant importance in biological systems. As an α-keto acid, the structure of pyruvate consists of a carbonyl group (C=O) that is located at the alpha site of its carboxylic group [47].

As the product of glycolysis, pyruvate is a central organic compound in the mixed-acid fermentation of glucose [48]. That is, this key intermediate metabolite is effectively a branching-point that can enter several different metabolic pathways and will thus lead to the formation of different intermediate/end-products, as dictated by the prevailing biological, environmental, thermodynamic and kinetic conditions of the system [49]. The central role of pyruvate in the mixed culture fermentation of complex organic

compounds can be appreciated in Figure 2-2. As per this figure, the range of potential intermediate products arriving from the primary fermentation of pyruvate may consist of oxidized and/or reduced metabolites, including the organic compounds acetate, propionate, lactate, n-butyrate and/or ethanol, as well as H_2 and/or CO_2 [49].

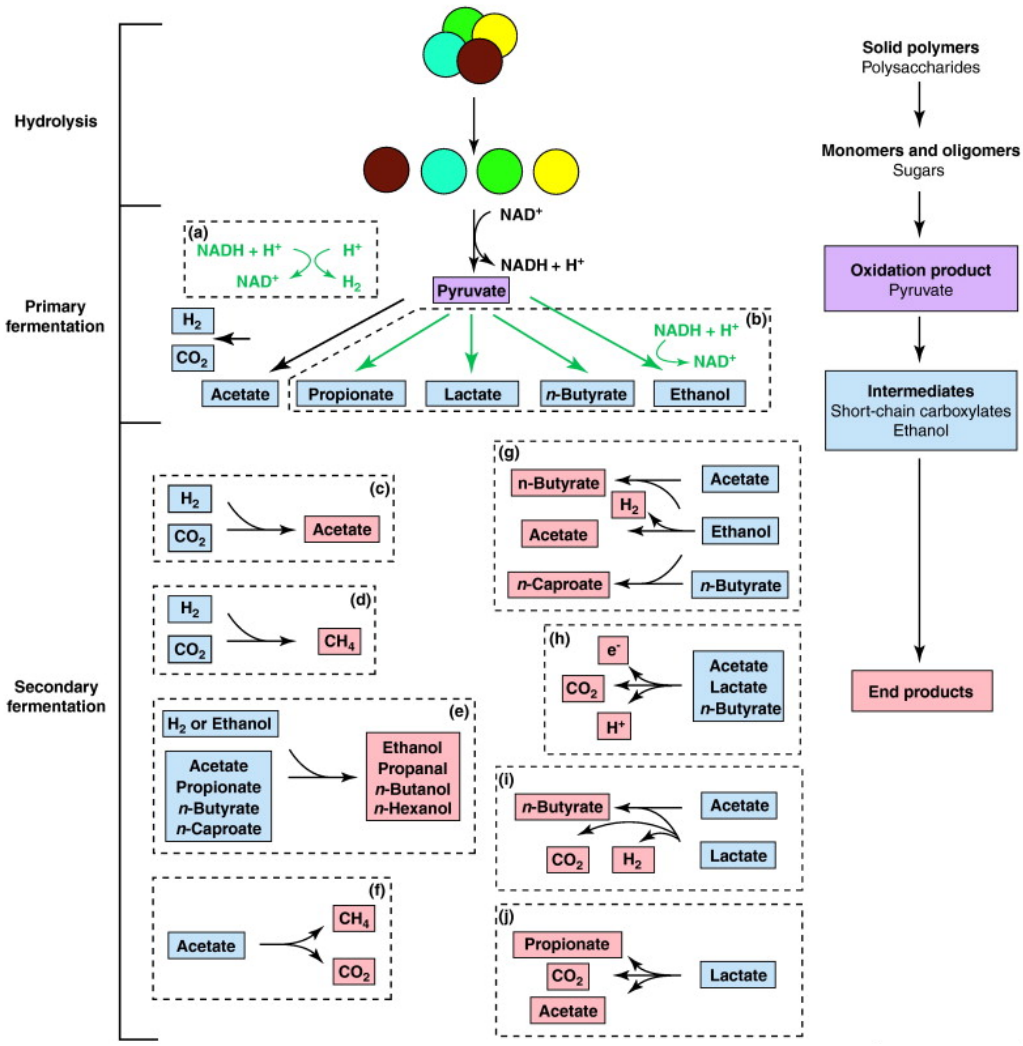

Figure 2-2. Pyruvate as a central metabolite in the fermentation of solid polymers by undefined mixed cultures (Source: Agler et al., 2011)

As a metabolic step that is coupled to re-oxidation of NADH via H+ reduction, the flow of electrons in the primary fermentation of pyruvate may proceed either (a) NADH oxidation; or (b) NADH oxidation via reduction of pyruvate or its oxidized organic derivatives, depending upon the hydrogen partial pressure [50]. At increasing hydrogen

partial pressures, the flow of electron from NADH shifts from H_2, acetate and CO_2 production towards formation of increasingly reduced fermentation products [51]. CO_2 and H_2 are produced in the pyruvate oxidation reaction that is catalyzed by pyruvate:ferredoxin oxidoreductase [49].

As depicted in Figure 2-2, the products of primary fermentation can react further within undefined mixed cultures through several secondary fermentation reactions: (c) autotrophic homoacetogenesis, (d) hydrogenotrophic methanogenesis, (e) carboxylate reduction to alcohols with hydrogen or ethanol, (f) acetoclastic methanogenesis, (g) chain elongation of carboxylates with ethanol, (h) electricigenesis, (i) lactate oxidation to n-butyrate (acetate and H^+ as electron acceptor), and (j) lactate reduction to propionate (oxidation to acetate for energy conservation) [49].

In this sense, elucidating the main drivers that influence the faith of pyruvate in mixed culture fermentation is of high scientific relevance in further exploring the potentials of anaerobic digestion technology, particularly in the development of applications aimed at steering end-product formation within these complex biochemical systems.

2.1.2. Relevance of butyrate as an intermediate metabolite in fermentation processes

While butyrate is one of the common products in the primary fermentation of a range of complex organic compounds –including glucose-, this carboxylic acid is also a key substrate that can be further degraded via secondary fermentation/acetogenesis and methanogenesis. Because understanding the potential faith of all target end products is an essential pre-requisite to maximizing production of VFA's via glucose fermentation, an assessment of the energetics and kinetics of the metabolic routes involved in butyrate degradation is a fundamental aspect of this study.

As presented in Eq. 2-1, the fermentative degradation of butyrate into acetate and hydrogen is energetically unfavorable under standard conditions and a pH of 7 (i.e. substrate and product concentrations of 1M, temperature 298 K, gas partial pressures of 1 atm):

$$CH_3CH_2CH_2COO^- + 2H_2O \rightarrow 2CH_3COO^- + H^+ + 2H_2 \quad \Delta G^{0'} = +48.1\ \text{kJ.mol}^{-1} \qquad \text{Eq. 2-1}$$

However, with efficient consumption of acetate and hydrogen by methanogenic archaea working in syntrophy with acetogenic bacteria, the biochemical oxidation of butyrate

into acetate and hydrogen becomes exergonic. For example, in anaerobic sludge digesters, while butyrate concentrations may amount to approximately 0.5 mM, actual acetate and H_2 concentrations are kept at around 1 mM and 2 Pa, respectively, which results in an actual Gibbs free energy change of -21 kJ.mol^{-1} for the reaction presented in Eq. 2-1 [29].

Although the fermentative oxidation of butyrate may be exergonic due to syntrophic bacterial/archaea interactions, the yield of energy of approximately -21 kJ.mol^{-1}, as obtained by substrate level phosphorylation, is still not sufficient to drive the synthesis of 1 ATP per mol of butyrate converted. In fact, under physiological conditions, and assuming a thermodynamic efficiency of 70% and ATP, ADP and Pi concentrations of 10 mM, 1 mM and 10 mM respectively, the free energy change needed for ATP synthesis has been suggested to amount to approximately 70 kJ.mol-ATP^{-1} [30].

According to Thauer and Morris (1984), in order to overcome this energetic limitation, a portion of the metabolic energy that is generated by substrate level phosphorylation (i.e. ATP) may be used to create a transmembrane electrochemical potential, which drives the thermodynamically unfavorable oxidation of butyryl-CoA to crotonyl-CoA, an important intermediate step in the oxidative conversion of butyrate to acetate. This mechanism, which corresponds to the occurrence of reverse electron transport (RET) coupled to butyryl-CoA oxidation, has been evidenced in the metabolism of e.g. the butyrate oxidizing bacteria *Syntrophomonas wolfei* [33].

While studies by Schink (1992, 1997) postulated that the minimum free energy quantum that would sustain microbial activity is in the order of -23 kJ.mol^{-1} [30, 31], various in situ measurements performed in lake sediments and anaerobic digesters with either defined cultures or anaerobic sludge have suggested that anaerobic fermentation of butyrate may proceed at free energy changes close to thermodynamic equilibrium (i.e. $\Delta G'$ close to 0 kJ.mol^{-1} butyrate) [34]. In proceeding close to thermodynamic equilibrium however, these biochemical conversions are highly susceptible to potential product inhibition; a form of negative feedback that impacts enzymatic activity and that has been recognized extensively in the literature [35, 36, 37, 38, 39, 40, 41, 42, 44, 45, 46, 47].

2.2. Anaerobic digestion for non-methane fermentations

CH_4 has been generally regarded as the most readily usable resource that can be recovered from the anaerobic degradation of complex organic wastes. In fact, anaerobic digestion for the production of methane is an excellent example of a process that is able

to combine stabilization of organic matter/waste with the production of a valuable end-product [22].

As an alternative to methane recovery, the process of anaerobic digestion of low value particulate feedstocks and/or wastewater may be shifted towards controlled accumulation and recovery of short chain fatty acids, the intermediate metabolites that are produced during the fermentation step [53]. These short chain fatty acids include volatile fatty acids (mainly acetate, propionate, butyrate), as well as lactate, and are conjunctively referred to as carboxylates. While the broth of unprocessed short-chain fatty acids does not hold a substantial economic value per se, after processing, these organic acids are intermediate building blocks that can be used in the production of higher value end-products [22]. According to the specific processing method, which may include organic acid concentration via membrane separation and/or further (bio)conversion to products that are more easily separated from the liquid stream, these building blocks may lead to attractive end-products including polyhydroxyalkanoates (PHA) and/or medium chain length fatty acids that have important industrial applications for the production of e.g. bio-plastic, lubricants, and fuels [52].

In order for anaerobic digestion to be effectively steered towards optimized production of organic acids, it is fundamental to consider that VFA's and other valuable medium-chain organic compounds may only dominate as end products provided methanogenesis is effectively inhibited. An example of an application where inhibition of methanogenic archaea is effectively achieved is the corn or sugar cane based production of bioethanol. In this specific case, production of biogas is prevented by very high concentrations of ethanol (the end product) [23].

In addition to end product inhibition, other environmental conditions may have a fundamental effect on steering end-product formation in anaerobic fermentation technologies from methane to other compounds, including carboxylates, and are worth evaluating in detail. Among others, parameters including pH [24], substrate concentration and feeding regime [23], temperature, oxygen availability, salinity or headspace composition may play a significant role in increasing the selectivity of undefined mixed culture fermentation [25].

Given anaerobic organic acid production relies on the fermentation of carbohydrates and protein derived amino acids, glucose, the model compound of cellulose, is one of the most important starting components for bio-based chemical synthesis. Thus, glucose can be considered as an adequate model feedstock in elucidating the mechanisms behind the product selectivity of mixed culture fermentations under a specific set of environmental variables [54]. Additionally, as a widely studied substrate, the metabolic pathways involved in glucose fermentation are well documented, allowing for further in-depth thermodynamic and kinetic analyses to be performed. In this sense, Figure 2-3 illustrates the major metabolic pathways involved in mixed culture glucose fermentation, including

the corresponding electron flows, key fermentation products, as well as formation of $NADH_2$, NAD^+, ADP and ATP [24].

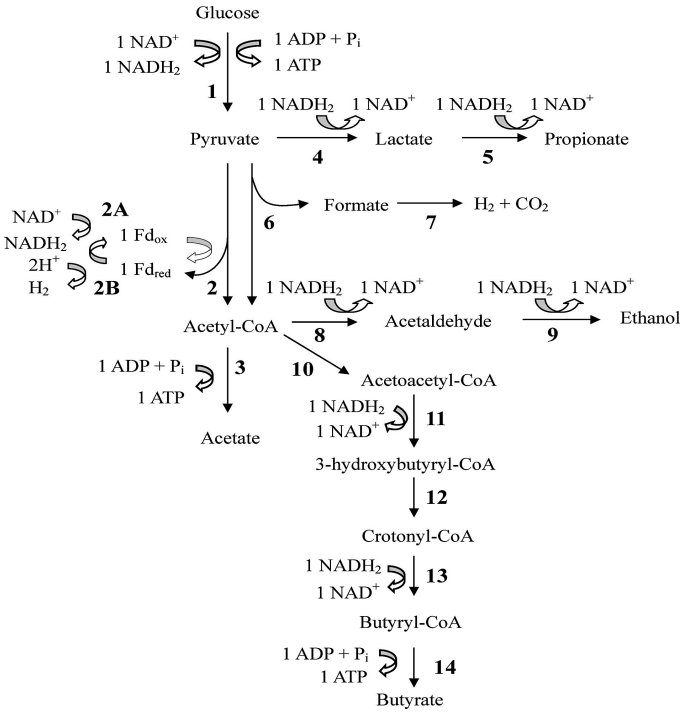

Figure 2-3. Metabolic pathways of mixed-acid fermentation of glucose. (*Prescott et al., 2002*)
*Note: ATP yields are based on 1 mol of the reaction product.

2.3. Anaerobic digestion at elevated pressure

2.3.1. Carbonate equilibrium and gas solubility at elevated CO_2 partial pressures

As described by Henry's law, the solubility of a given gas is directly proportional to the partial pressure of the gas in question. For example, for a given partial pressure of CO_2, the theoretical amount of dissolved CO_2 can be determined with Eq. 2-2.

$$[H_2CO_3] = K_{H,CO_2} * pCO_2$$ Eq. 2-2

Where:

- $[H_2CO_3]$: Concentration of dissolved CO_2 [$mol.l^{-1}$]
- $K_{H,CO2}$: Henry's law solubility constant for CO_2 [= 0.318 $mol.l^{-1}.MPa^{-1}$ at 298 K]
- pCO_2 : partial pressure of CO_2 in the gas phase

As implied by Eq. 2-2, when dissolved CO_2 reacts with water, carbonic acid (i.e. H_2CO_3) is formed. Thus, it can be deduced that elevated CO_2 partial pressures can lead to a decrease in the solution's pH and a certain extent of broth acidification, with the potential to hinder the occurrence of pH dependent biochemical conversions, including methanogenesis [24].

The relative activities of each of the species of relevance in the carbonate system (i.e. CO_2 and/or H_2CO_3, HCO_3^-, CO_3^{2-}) are described by the following apparent dissociation constants:

$$K_H = \frac{[H_2CO_3^*]}{[CO_2]} = 10^{-1.47}$$ Eq. 2-3

$$K_1 = \frac{[H^+]*[HCO_3^-]}{[H_2CO_3^*]} = 10^{-6.3}$$ Eq. 2-4

$$K_2 = \frac{[H^+]*[CO_3^{2-}]}{[HCO_3^-]} = 10^{-10.25}$$ Eq. 2-5

$$K_w = \frac{[H^+]*[OH^-]}{[H_2O]} = 10^{-14}$$ Eq. 2-6

In addition to the carbonate equilibrium taking place in accordance with these dissociation constants, the alkalinity or acid neutralizing capacity (ANC) of the solution is an extra parameter that dictates the overall reactor acidity under elevated CO_2 partial pressures. As presented in Eq. 2-7, this acid neutralizing capacity can be defined as the excess of cations of strong bases in relation to the concentration of anions of strong acids in solution [55, 56]. Alternatively, this alkalinity/ANC can be expressed in terms of the concentration of the ions in Equations 2-4, 2-5 and 2-6, plus the concentration of any dissociated organic acids (i.e. $[OA^-]$) that may be present in solution (Eq. 2-8).

$$[ANC^-] = [Na^+] + [K^+] + 2[Ca^{2+}] + 2[Mg^{2+}] + [NH_4^+] - [Cl^-] - 2[SO_4^{2-}] - 3[PO_4^{3-}]$$ Eq. 2-7

$$[ANC^-] + [H^+] = [HCO_3^-] + 2[CO_3^{2-}] + [OH^-] + [OA^-] \quad \text{Eq. 2-8}$$

From Eq. 2-7 and Eq. 2-8, it can be deduced that the acid neutralizing capacity is a quantity that is intrinsically related to the solution's charge balance. Thus, it is expected that a useful expression that relates the concentration of ions of strong bases/acids, to the concentration of dissociated organic acids in solution can be derived by combining these two expressions. As a means of simplifying Eq. 2-8, it is of relevance to note that in developing the present experiments the pH values ranged between 6-8 under all conditions tested. With pH values within this range, the relative concentrations of CO_3^{2-}, OH^- and H^+ were more or less negligible. Under these operational conditions, Eq. 2-8 can be simplified to:

$$[ANC^-] = [HCO_3^-] + [OA^-] \quad \text{Eq. 2-9}$$

Similarly, with consideration to the composition of the basal medium that was used in these experiments, as described in Section 3.3, the charge due to ions other than Na^+ was negligible. As such, Eq. 2-7 can be simplified to:

$$[ANC^-] = [Na^+] \quad \text{Eq. 2-10}$$

Combining Eq. 2-9 and Eq. 2-10, and replacing [OA-] by the concentrations of either pyruvate or butyrate as the organic acids of concern in the present investigation yields:

$$[Na^+] = [Pyruvate^-] + [HCO_3^-] \quad \text{Eq. 2-11}$$

$$[Na^+] = [Butyrate^-] + [HCO_3^-] \quad \text{Eq. 2-12}$$

Hence, after full conversion of pyruvate and/or butyrate in each of the experiments, the ANC is only dictated by the bicarbonate concentration in each case.

An expression for the total inorganic carbon (TIC) balance, as a function of the ANC and the solution's pH, can be thus derived by combining Eq. 2-11/Eq. 2-12 with the expressions for the carbonate equilibrium in Eq. 2-2 through Eq. 2-6. With pH values in the range 6-8, the TIC balance would correspond to:

$$TIC = HCO_3^- + CO_2(aq.) + CO_2(g)$$ Eq. 2-13

or, equivalently:

$$TIC = (ANC) + \frac{(ANC)*10^{-pH}}{K_1} + \frac{(ANC)*10^{-pH}\,V_g}{K_1\,K_{HCO_2}\,V_l*R*T}$$ Eq. 2-14

Where, ANC is given in meq.l^{-1}, $K_1 = 10^{-pKa}$, $K_{HCO2} = 10^{-6.55}$ mol.l^{-1}.Pa^{-1}, V_l = liquid volume in l, V_g = gas volume in l, T = 308.15 K and R = 8.3145 10^3 l.Pa.K^{-1}.mol^{-1}.

2.4. Thermodynamics of (bio)chemical reactions

A broad theoretical assessment of the feasibility of a specific biochemical conversion can be easily achieved by calculating the change in Gibbs free energy of the reaction in question. Under standard conditions (i.e. 298K, 1 M substrates and products, 1 atm. gas pressure), this thermodynamic potential can be determined via Eq. 2-15.

$$\Delta G^0 = \sum_{i=1}^{n} Y_i * G_f^0$$ Where: Eq. 2-15

- ΔG^0: free energy change at standard conditions
- Yi: stoichiometric coefficient of the substrates (-) and products (+) in the reaction
- ΔG_f^0: standard free energy of formation of the compounds in the reaction

In order to assess the thermodynamic favorability of a biochemical reaction at physiologically viable conditions, the change in Gibbs free energy at standard conditions but a pH of 7 [H^+] = 1 x 10^{-7} M instead of 1 M) can be calculated via Eq. 2-16.

$$\Delta G^{0\prime} = \Delta G^{0} + R.T_s.\ln[(1*10^{-7})^{Y_H}]$$ Eq. 2-16

Where:

- $\Delta G^{0'}$: free energy change at standard conditions but pH 7
- ΔG^{0}: free energy change at standard conditions
- R: gas constant (8.314 $J.mol^{-1}.K^{-1}$)
- Ts: Standard temperature in Kelvin = 298K
- Y_H: stoichiometric coefficient of the H^+ ion ((-) if substrate and (+) if product in the reaction)

Based on the Gibbs free energy change at the standard environmental conditions (ΔG^0, with $[H^+]$ = 1M), and taking aceticlastic methanogenesis as an example, the corresponding driving force at actual conditions of temperature, pH and activities of substrates and products can be determined with Eq. 2-17.

$$\Delta G = \Delta G^{0} + RT\ ln\frac{pCH_4 * pCO_2}{[Ac^-]*[H^+]}$$ Eq. 2-17

Where:

- ΔG: actual free energy change
- R: gas constant (8.314 $J.mol^{-1}.K^{-1}$)
- T: temperature in Kelvin
- pCH_4, pCO_2: gas pressure of CH_4 and CO_2
- [Ac-], $[H^+]$: molar concentrations of acetate and hydrogen ions

3. MATERIALS AND METHODS

3.1. Inoculum

The microbial culture used in these experiments consisted of flocculent anaerobic sludge sourced from a full-scale anMBR application treating wastewater from the food industry.

This particular mixed culture of fermentative, acetogenic and methanogenic bacteria and archaea evidenced a relative tolerance for elevated pressures as high as 8.0 bar, as tested in the present set of experiments. A summary of the main characteristics of this mixed culture consortium is provided in Table 3-1.

Table 3-1. Physico-chemical characterization of the Inoculum

Parameter	UoM	Value		
		Range	Mean	SD
TCOD	g/l	21.88 – 22.82	22.22	0.52
SCOD	g/l	1.87 – 1.94	1.92	0.04
TOC	g/l	7.13 – 8.66	7.72	0.83
TSS	g/l	15.81 – 15.95	15.87	0.07
VSS	g/l	13.56 – 13.67	13.62	0.06
VSS/TSS	%	85.73 – 85.90	85.80	0.09
NH_4-N	mg/l	105 – 109	107	2.00
TP	mg/l	111 – 113	112	0.90
pH	-	-	7.3	-

3.2. Experimental set-up

The present laboratory scale trials were conducted as two sets of 5 experimental treatments in batch mode, aimed at evaluating the degradation of 2 specific substrates (i.e. butyrate and pyruvate). Each of these sets of experiments evaluated butyrate and pyruvate degradation at 5 different initial CO_2 partial pressures, namely 0.2, 1.0, 3.0, 5.0 and 8.0 bar. Following Henry's Law, varying amounts of CO_2 migrated and dissolved into the liquid phase in each case, until the corresponding equilibrium pressures presented on Table 3-2 were reached.

Table 3-2. Experimental CO_2 partial pressures at equilibrium

Set of Experiments	**pCO_2** [**Initial** / *Equilibrium*] [bar]				
	0.2	**1.0**	**3.0**	**5.0**	**8.0**
Pyruvate Experiments	*0.2*	*1.0*	*1.3*	*1.9*	*3.3*
Butyrate Experiments	*0.2*	*1.0*	*1.5*	*2.0*	*3.5*

All experiments were conducted at mesophilic conditions and at a constant temperature of 35 ±1˚C (i.e. 308.15 K). Constant temperature and homogeneous mixing were achieved by means of either an incubator shaker operated at approximately 115 rpm (i.e. Brunswick Innova® 44/44R, Eppendorf, United States), or a static incubator (i.e. Thermo Scientific, France) fitted with a rotary shaker, which was operated at 70 rpm (i.e. LAB Associates, The Netherlands).

According to the gas pressure at start-up (i.e. pCO_2 tested), two different types of experimental set-ups were implemented:

i. Experiments at atmospheric pressure (i.e. batch trials at 0.2 and 1.0 bar pCO_2): these sets of experiments were performed in 250 ml Duran glass bottles, air-tight sealed with rubber stoppers. With consideration to the physico-chemical characteristics of the anaerobic biomass, the reactors were operated at liquid working volumes of 150 ml. Figure 3-1 provides a schematic representation of the experimental set-up that was used in developing the batch experiments at atmospheric pressure.

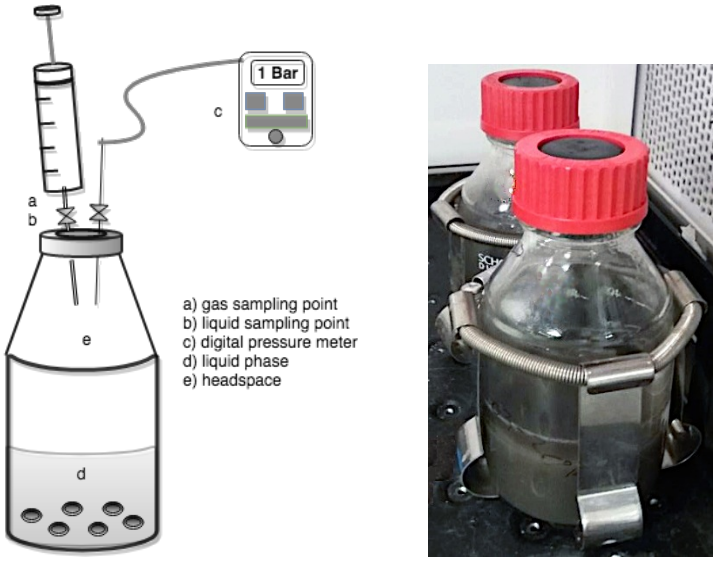

Figure 3-1. Schematic representation of the experimental set-up for batch experiments conducted at 0.2 and 1 bar pCO_2

ii. Experiments at pressurized conditions (i.e. batch trials at 3.0, 5.0 and 8.0 bar pCO_2): these experiments were conducted in pressure resistant stainless-steel vessels with a total volume of 200 ml. These reactors were fitted with liquid and gas sampling ports, as well as either manual glycerin manometers (T-meter®, France) or digital pressure sensors (B+B Thermo-Techniek, Germany). The pressurized experiments were conducted with a liquid working volume of either 120 or 150 ml. A schematic representation of the corresponding set-ups that were implemented in conducting batch experiments at 3.0, 5.0 and 8.0 bar pCO_2 is provided in Figure 3-2.

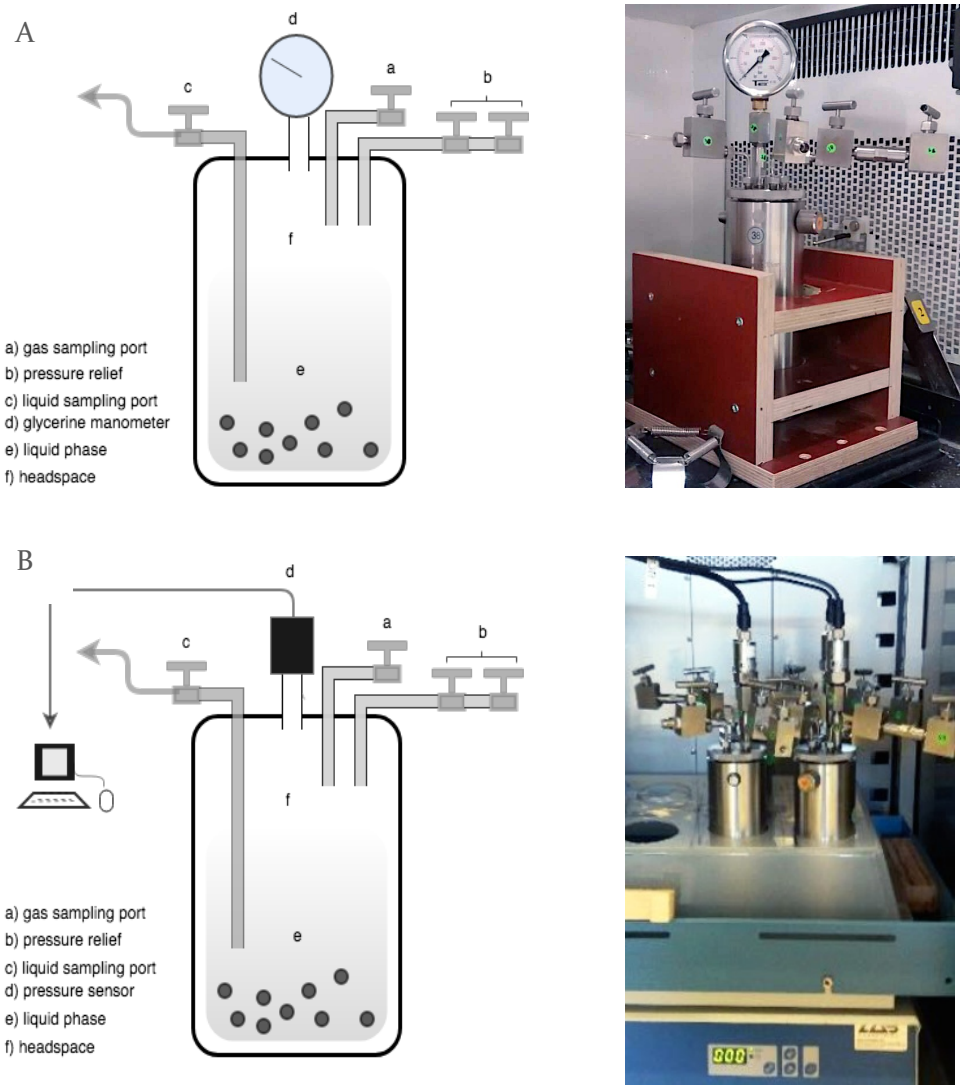

Figure 3-2. Schematic representation of the experimental set-up for batch experiments conducted at 3.0, 5.0 and 8.0 bar pCO_2. (A) Reactors fitted with glycerin manometers. (B) Reactors fitted with pressure sensors.

3.3. Reactor operation

The present batch experiments were performed at liquid to gas ratios of 1.5:1 or 3:1. Similarly, a constant substrate to biomass ratio of 1:2 (i.e. COD:VSS) was used in all of the trials. Based on these ratios, as well as on the working liquid volumes for the atmospheric and pressurized experiments, the VS fraction of the inoculum and a target substrate concentration of approximately 1 g $COD.l^{-1}$, the corresponding quantities of inoculum and substrate that were used in each of the experiments were determined and have been summarized in Table 3-3. Additionally, in order to promote adequate bacterial metabolic activity, the substrate medium was provided with 6 $ml.l^{-1}$ of a macro-nutrient solution as described in Table 3-4, as well as 0.6 $ml.l^{-1}$ of a trace element solution with a composition as shown in this table.

Table 3-3. Overview of the experimental trials

Set of Experiments	Exp. Nr*.	pCO_2 [bar]		Exp. Duration [h]	Initial Substrate Concentration [g $COD.l^{-1}$]	Liquid Volume [l]		Gas Volume** [l]
		Start-up	Equil.			Substrate Medium	Biomass	
Pyruvate Experiments	1	0.2	0.2	377	1.0	0.13	0.02	0.10
	2	1.0	1.0	140	1.0	0.13	0.02	0.10
	3	3.0	1.3	377	1.0	0.13	0.02	0.05
	4	5.0	1.9	377	1.0	0.13	0.02	0.05
	5	8.0	3.3	377	1.0	0.13	0.02	0.05
Butyrate Experiments	6	0.2	0.2	281	1.1	0.13	0.02	0.10
	7	1.0	1.0	281	1.1	0.13	0.02	0.10
	8	3.0	1.5	305	1.1	0.10	0.02	0.08
	9	5.0	2.0	332	1.1	0.10	0.02	0.08
	10	8.0	3.5	332	1.1	0.10	0.02	0.08

** In order to allow evaluation of the statistical significance of the experimental outputs, each of the 10 substrate/pCO_2 scenarios were run in triplicate. In this sense, a total of 30 experimental units were set-up and monitored during the course of this investigation.*

*** Water is assumed uncompressible and thus the gas volume corresponds to the total reactor volume minus the working liquid volume.*

Table 3-4. Composition of the macro and micro-nutrient stock solutions

Macronutrients (6 ml.l^{-1})		**Trace Elements (0.6 ml.l^{-1})**			
Compound	**Concentration (g.l^{-1})**	**Compound**	**Concentration (g.l^{-1})**	**Compound**	**Concentration (g.l^{-1})**
NH_4Cl	170	$FeCl_3.4H_2O$	2	$NiCl_2.6H_2O$	0.05
$CaCl_2.2H_2O$	8	$CoCl_2.6H_2O$	2	EDTA	1
$MgSO_4.7H_2O$	9	$MnCl_2.4H_2O$	0.5	$ZnCl_2$	50
		$CuCl_2.2H_2O$	30	HBO_3	0.05
		$(NH_4)6Mo7O_2.4H_2O$	0.09	HCl 36%	1 ml.l^{-1}
		$Na_2SeO_3.5H_2O$	0.1		

** Additionally, the trace element stock solution contains yeast extract and resazurine at concentrations of 2 g.l^{-1} and 0.5 g.l^{-1}, respectively.*

In order to limit acidification in the reactors, the liquid medium for all of the experiments was also provided with a concentration of 100 mM of sodium bicarbonate ($NaHCO_3$).

Based on the equilibrium pCO_2 presented in Table 3-2, the addition of this amount of $NaHCO_3$ (i.e. 0.1 M), the apparent dissociation constant of carbonic acid (i.e. K_1 in Eq. 2-4) corrected for the experimental temperature of 35˚C (i.e. $K_{1,\,(35^\circ C)} = 5.5x10^{-7}$), Henry's solubility constant for CO_2 (i.e. K_H in Eq. 2-2) at 35˚C (i.e. $K_{H,\,(35^\circ C)} = 0.026$ mol.l^{-1}.bar^{-1}) and an initial pH of the un-buffered liquid medium equal to 7.0 (i.e. [H+] = 1.0 x 10^{-7} M), the equilibrium pH for each of the batch experiment were determined via Eq. 3-1/Eq. 3-2 below and are presented in Table 3-5.

$$pH = (-\log_{10} k_{1,\_35^\circ C}) + \left(\log_{10} \left[\frac{[HCO_3^-]}{[H_2CO_3^*]}\right]\right) \quad \text{Eq. 3-1}$$

with,

$$[H_2CO_3^*] = \left(pCO_{2\_Eqilibrium} * K_{H,35^\circ C}\right) + \left(\frac{[H^+]*[HCO_3^-]}{K_{1,35^\circ C}}\right) \quad \text{Eq. 3-2}$$

Table 3-5. Initial/equilibrium pH of the liquid broth with addition of 100 mM $NaHCO_3$

Set of Experiments	Exp. Nr*.	$NaHCO_3$ [M]	K_1 (35 °C)	K_H (35 °C) [$mol.l^{-1}.bar^{-1}$]	$[H^+]$ (pH = 7) [M]	pCO_2 [bar]	Equilibrium pCO_2 [bar]	Equilibrium pH
Pyruvate Experiments	1	0.1	5.54×10^{-7}	0.026	1.0×10^{-7}	0.2	0.2	6.9
	2					1.0	1.0	6.6
	3					3.0	1.3	6.5
	4					5.0	1.9	6.4
	5					8.0	3.3	6.2
Butyrate Experiments	6	0.1	5.54×10^{-7}	0.026	1.0×10^{-7}	0.2	0.2	6.9
	7					1.0	1.0	6.6
	8					3.0	1.5	6.5
	9					5.0	2.0	6.4
	10					8.0	3.5	6.2

Figure 3-3 below provides a graphical depiction of the influence of increasing CO_2 partial pressures on the pH of the liquid broth, as per the values that have been presented in Table 3-5.

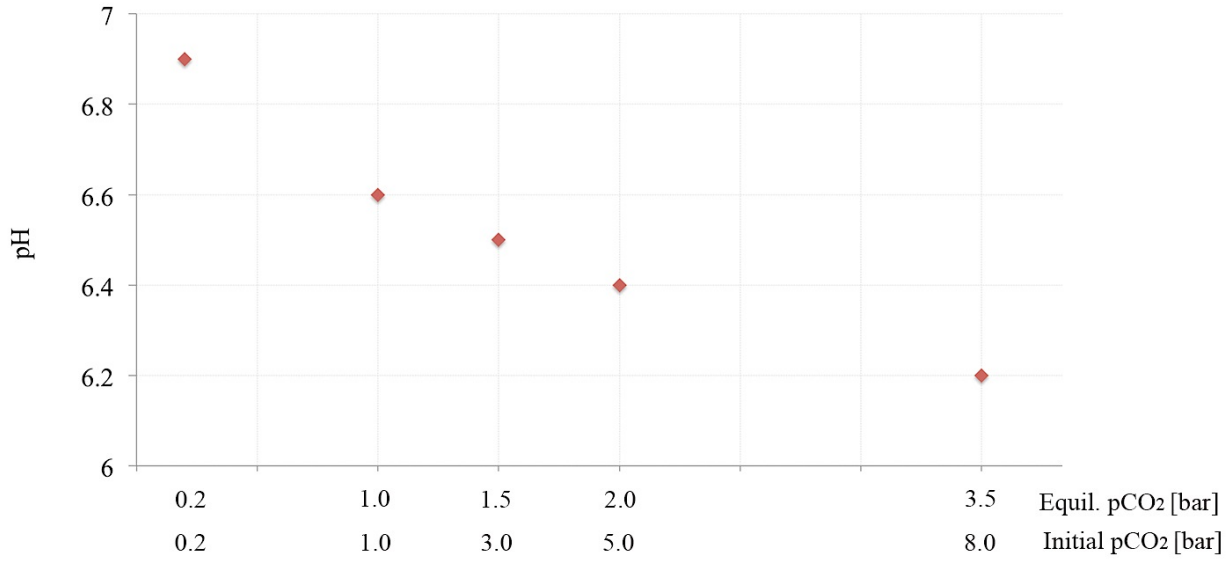

Figure 3-3. Changes in the liquid broth's pH in response to the operating/equilibrium CO_2 partial pressures

3.4. Analytical methods

3.4.1. Composition of the liquid phase

In order to monitor the conversion of the substrate in time, 2 ml liquid samples were collected from each of the reactors twice a day on the first day of the experiments, daily between days of operation 2 and 4, and then once every 2 days from day of operation 5 until experiment completion.

Each of the samples was prepared for further analysis by centrifugation at 14,500 rpm for 5 minutes, followed by filtration with 0.45 µm polyethersulfone filters (Chromafil®, Germany). The filtered samples were refrigerated for a maximum of 5-8 days before being diluted 1:1 with pentanol and acidified with formic acid, in accordance with the protocol by *Zhang et al.* [57]. Acidified samples were then analyzed for their content of VFA's by gas chromatography (7890A GC, Agilent Technologies with flame ionization detector (FID) operated at 240˚C, oven temperature of 80˚C, injection temperature of 120˚C and an Agilent 19091F-112 (25m x 0.32mm x 0.5µm) glass column. Helium was used as the carrier gas at a constant flow of 2.4575 $ml.min^{-1}$).

3.4.2. Composition of the gas phase

Gas samples of 5 ml were collected from each of the reactors using air-tight syringes every 3 to 5 days starting from the moment of pCO_2 equilibration, 1 to 2 hours after experiment start-up. Relative gas composition at atmospheric conditions was subsequently determined via gas chromatography (7890A GC, Agilent Technologies), operated at an oven temperature of 45˚C, by directing the samples over an Agilent HP-PLOT Molesieve GC column (30m x 0.53 mm x 25 µm) with helium as the carrier gas, which was provided at a constant flow of 10 $ml.min^{-1}$. Detection took place by a thermal conductivity detector (TCD) operated at 200˚C.

3.4.3. Total and volatile suspended solids

Determination of total and volatile suspended solids (i.e. TSS and VSS) of the inoculum prior to reactor inoculation and of the liquid broth at the end of the experiments were measured following Standard Methods [58].

3.4.4. Chemical Oxygen Demand

Determination of the soluble COD was performed on pre-filtered liquid samples (i.e. 0.45 µm polyethersulfone filters, Chromafil®, Germany) collected at the end of each of the batch experiments. COD analyses were conducted in accordance to standard ISO 6060-1989 and DIN 38409-H41-H44 methods using HACH COD cuvette tests and a DR 3900 bench top spectrophotometer.

COD balances were determined by means of Eq. 3-3. With consideration to the relatively short duration of the batch experiments, biomass growth was expected to be very limited and this term was thus not considered in formulating the COD balances.

$$COD_{substrate} = COD_{VFAs} + COD_{CH_4} + [COD_{soluble} - COD_{VFAs}] \quad \text{Eq. 3-3.}$$

4. RESULTS AND DISCUSSION

Methane, one of the common end products in the anaerobic degradation of organic compounds, was observed as a predominant electron sink in all of the experiments conducted as part of this study. While methane production accounted for 35 ± 22% - 68 ± 3.0% of the COD in the pyruvate experiments at pCO_2's of 3.0 and 0.2 bar respectively, between 11 ± 2.0% - 74 ± 19% of the initial COD in the butyrate trials was mineralized into CH_4 by the end of the 8.0 and 3.0 bar pCO_2 experiments, respectively. Even though CH_4 was a dominant end compound in all of the pyruvate and butyrate degradation tests, the results from this investigation suggest that increasing pCO_2 conditions in the reactors steered, to a great extent, product formation towards the prevalence of intermediate compounds arriving from CO_2 consuming (-carboxylation-) steps.

Thus, in addition to acetate and hydrogen formation, as the main precursors to methane formation in these experiments, prevailing CO_2 partial pressures appear to have had an influence on the yield and/or accumulation of other organic compounds, particularly propionate.

4.1. Product Spectrum

4.1.1. End products and intermediate metabolites in pyruvate degradation

Figure 4-1 provides an overview of the key (intermediate) products of the fermentative degradation of pyruvate that were identified under the experimental conditions tested, corresponding to variable CO_2 partial pressures of between 0.2 – 8.0 bar. The relative abundance of the main metabolites that were recorded over the course of the experiments were quantified in terms of their average COD equivalence, as a fraction of the initial COD-pyruvate that was provided at start-up.

While a total of five different CO_2 partial pressures were tested, namely 0.2, 1.0, 3.0, 5.0 and 8.0 bar, following Henry's Law, these partial pressures of CO_2 equilibrated rapidly to 0.2, 1.0, 1.3, 1.9 and 3.3 bar, respectively. With the equilibrium pCO_2's as the starting point, variations in the CO_2 partial pressures were recorded over time and are also presented in these figures. Having performed each of the batch experiments in triplicate,

the standard deviations of the most abundant compounds that were identified are also shown in Figure 4-1. With a headspace composition of 80% N_2 : 20% CO_2, the batch experiments that were run at 0.2 pCO_2 were used as the experimental blanks. Thus, the results from this set of experiments served as a base for comparison and assessment of the outputs from all other pCO_2 conditions evaluated.

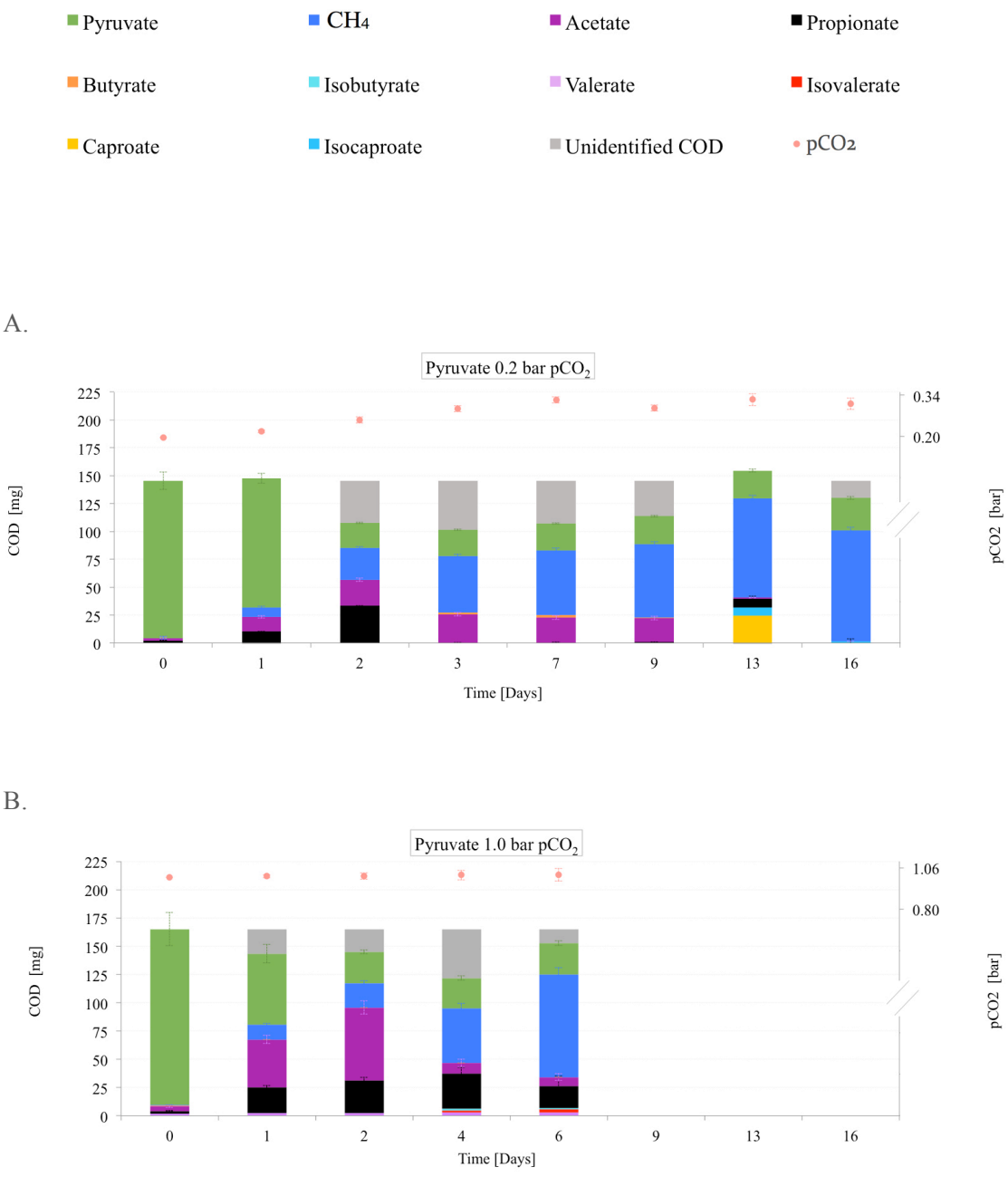

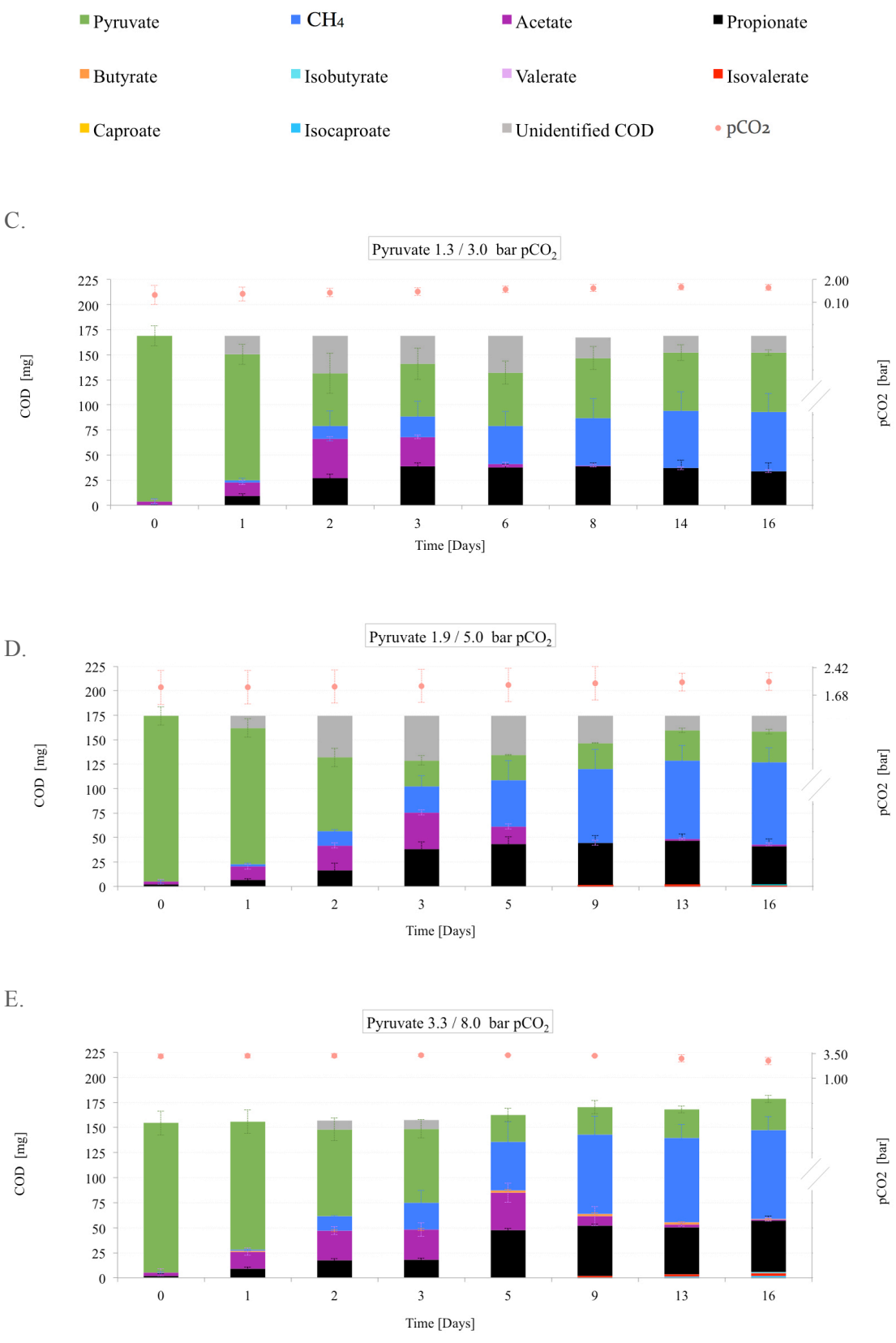

Figure 4-1. Product spectrum in the fermentative degradation of pyruvate at 5 different CO_2 partial pressures: (A). 0.2 bar; (B). 1.0 bar; (C). 3.0 bar; (D). 5.0 bar; (E). 8.0 bar

Table 4-1 provides an overview of the relative abundance of the main electron sinks that were identified at the end of the pyruvate experiments, for each of the CO_2 partial pressures tested. This information has also been depicted in Figure 4-2.

Table 4-1. Fractions of electron sinks at different pCO_2 conditions at the end of the pyruvate degradation experiments

Compound	**Initial pCO_2 [pH]**				
	0.2 [6.9]	**1.0 [6.6]**	**3.0 [6.5]**	**5.0 [6.4]**	**8.0 [6.2]**
% CH_4	68 ± 3.0	55 ± 6.0	35 ± 22.0	48 ± 18.0	54 ± 16.0
% Acetate	FD*	5 ± 1.9	FD	1 ± 0.5	1 ± 0.4
% Propionate	**FD**	**12 ± 5.6**	**20 ± 4.8**	**23 ± 4.0**	**31 ± 9.0**
% Butyrate	FD	FD	-	-	<1 ± 0.1
% Isobutyrate	-	<1 ± 0.1	-	<1 ± 0.1	<1 ± 0.1
% Valerate	-	2 ± 0.2	-	-	-
% Isovalerate	-	2 ± 0.2	FD	1 ± 0.8	2 ± 0.2
% Caproate	FD	-	-	-	-
% Isocaproate	1 ± 0.8	-	-	-	1 ± 0.1
% Residual pyruvate**	*20 ± 4.7*	*17 ± 8.0*	*35 ± 14.0*	*18 ± 7.0*	*19 ± 12.0*
% Unidentified COD (e.g. new biomass)	11 ± 4.6	7 ± 2.8	10 ± 4.5	9 ± 4.5	FD

**FD = Fully Degraded (This metabolite was fully degraded by the end of the experiment).*

***Although the data provided in Table 4-1 suggests an apparent persistence of an amount of un-degraded pyruvate by the end of all of this set of experiments, it is believed that the amounts of pyruvate recorded by the end of the trials may reflect a systematic measurement error in the HPLC, as opposed to reflecting an actual trend for the occurrence of incomplete pyruvate degradation.*

**** Although H_2 was an additional intermediate electron sink formed via oxidation of pyruvate into acetate, H_2 partial pressures remained below the GC's detection limit at all times for all of the experiments (< 60 Pa pH_2). H_2 was consumed effectively via the formation of propionate, butyrate and/or methane in the pyruvate experiments.*

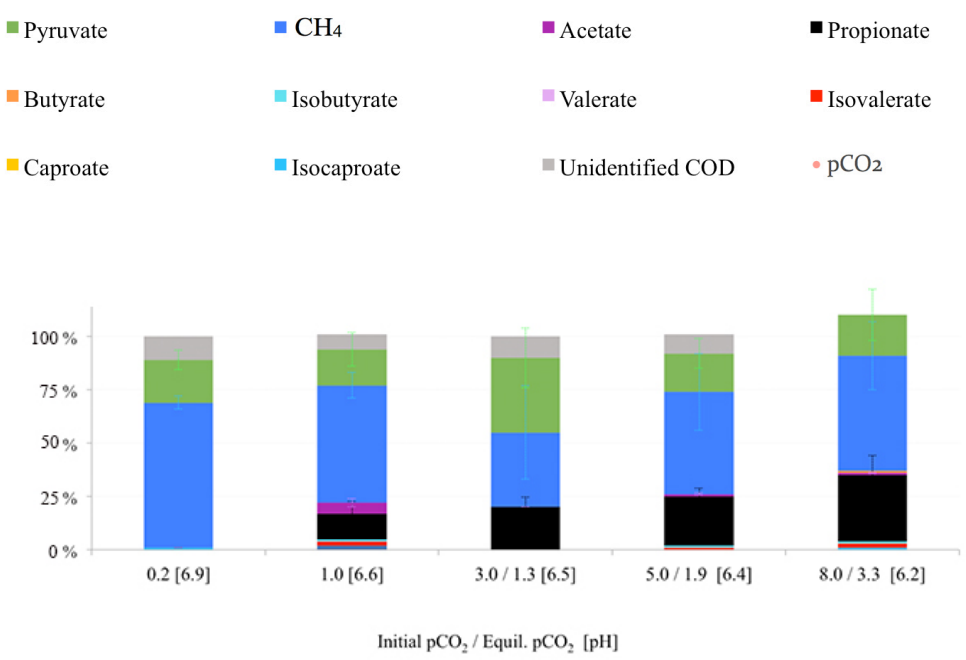

Figure 4-2. Overview of the product spectrums at 5 different CO_2 partial pressures at the end of the pyruvate experiments

In assessing the range of products that were formed at different pCO_2's against the outputs of the "blank"/0.2 pCO_2 experiments, increasing CO_2 partial pressures up to 8.0 bar appear to have had a discrete detrimental impact on the formation of acetate -via acetogenesis-, with the flow of electrons in pyruvate shifting away from this decarboxylation step towards preferential CO_2 utilizing metabolic routes. In this sense, excess CO_2 availability in the system promoted enhanced propionate formation via succinate, as a carboxylation step that consumes CO_2 (i.e. the proportion of Propionate-COD that accumulated in the reactors by the end of the experiments increased from 12 ± 5.6% when operating at 1.0 bar pCO2 up to 31 ± 9.0% for the experiments conducted at 8.0 bar pCO_2). Thus, the yields of propionate formation via pyruvate fermentation exhibited an increasing trend in response to elevated CO_2 partial pressures, with values for these yields estimated at 0.24 ± 0.01, 0.24 ± 0.01, 0.26 ± 0.01 and 0.34 ± 0.01 mgPropionate-COD.mg^{-1}Pyruvate-COD for pCO_2's of 0.2, 3.0, 5.0 and 8.0 bar, respectively.

As observed from Figure 4-1, while the amounts of propionate that were formed at low CO_2 partial pressures of 0.2 bar further degraded into acetate and CH_4, higher levels of dissolved CO_2 in the reactors (i.e. pCO2's of 3.0, 5.0 and 8.0 bar) led to propionate accumulation in the systems. Considering that the degradation of propionate via acetate formation also constitutes a decarboxylation step and thus not provide a mechanism for

effective use of excess CO_2, higher dissolved CO_2 concentrations appear to have hindered the propionate degradation pathway thus leading to the accumulation of this metabolite in the reactors.

While very limited amounts of butyrate were formed during the pyruvate fermentation experiments at pCO_2's of 0.2, 1.0 and 8.0 bar, no clear trend was observed that allows the derivation of hard conclusions regarding the impact of elevated CO_2 partial pressures on the metabolic route of pyruvate into butyrate.

4.1.1.1. Main catabolic pathways in the fermentative degradation of pyruvate

Based on the range of products that were identified in the pyruvate experiments, it is hypothesized that the major catabolic pathways that were involved in the anaerobic degradation of pyruvate at varying pCO_2's are as presented in Figure 4-3.

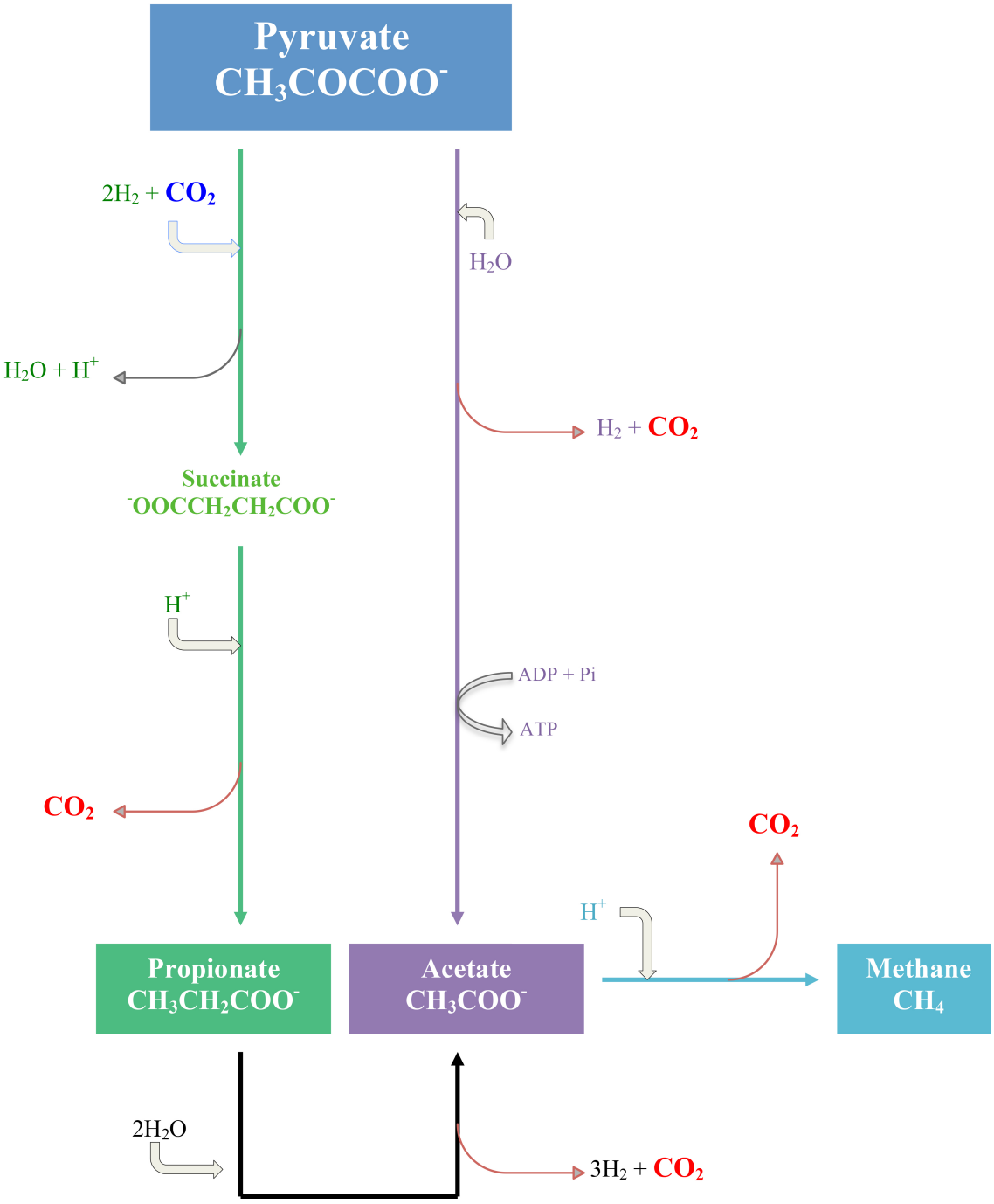

Figure 4-3. Major catabolic pathways involved in the anaerobic degradation of pyruvate at varying CO_2 partial pressures

As presented in Figure 4-3, ATP is only synthesized within two of the main pyruvate fermentation pathways, namely during the formation of acetate and butyrate. With very limited butyrate produced (i.e. <0.1 mM), it can be inferred that substantial amounts of ATP in the pyruvate experiments were only synthesized via acetate formation, by means of substrate level phosphorylation. Similarly, synthesis of reducing power (i.e. denoted as H_2 in Figure 4-3) in the pyruvate experiments solely took place during oxidation of pyruvate into acetate via Acetyl-CoA.

Based on these observations, it appears that in the absence of any other external electron donors/source of reducing power, the fermentative degradation of pyruvate into either propionate or butyrate will be necessarily coupled to pyruvate oxidation via acetate production. Thus, in the presence of elevated pCO_2's, any available reducing power, however limited, was increasingly steered towards propionate production, as a carboxylation reaction that allows consumption of excess CO_2.

4.1.2. End products and intermediate metabolites in butyrate degradation

Figure 4-4 provides an overview of the product spectrum of the anaerobic degradation of butyrate under different CO_2 partial pressures of 0.2, 1.0, 3.0, 5.0 and 8.0 bar, as recorded over the course of the batch experiments. Shortly after start-up, and in accordance with Henry's Law, these initial CO_2 partial pressures equilibrated to 0.2, 1.0, 1.5, 2.0 and 3.5 bar, respectively. In addition to the evolution of the relative pCO_2 over time, standard deviations of the main metabolites and/or end products have also been depicted in Figure 4-4. The butyrate batch experiments that were run at 0.2 pCO_2 (i.e. headspace composition of 80% N_2 : 20% CO_2) were used as the experimental blanks.

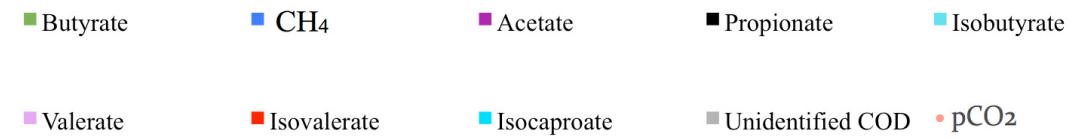
Butyrate
CH4
Acetate
Propionate
Isobutyrate
Valerate
Isovalerate
Isocaproate
Unidentified COD
pCO2

A.

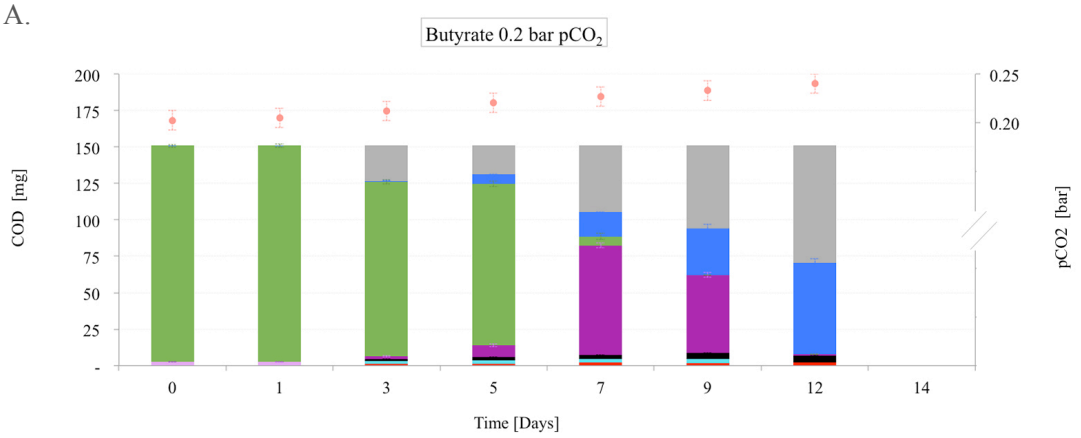
Butyrate 0.2 bar pCO2
COD [mg]
pCO2 [bar]
Time [Days]

B.

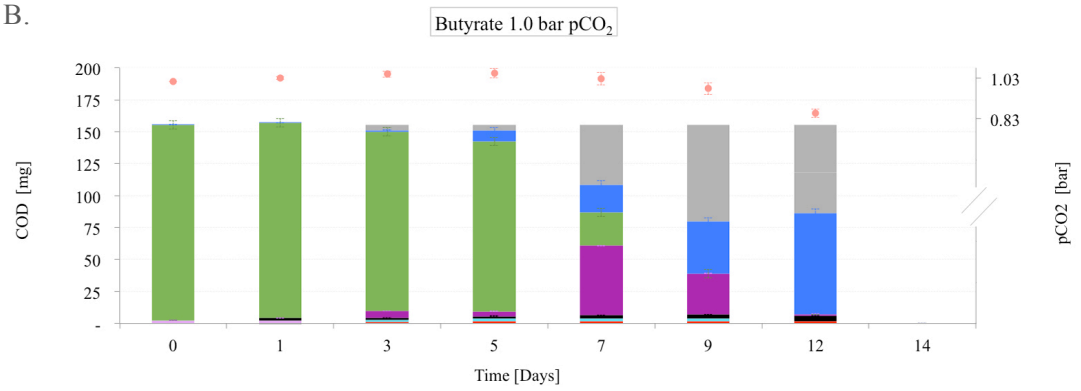
Butyrate 1.0 bar pCO2
COD [mg]
pCO2 [bar]
Time [Days]

C.

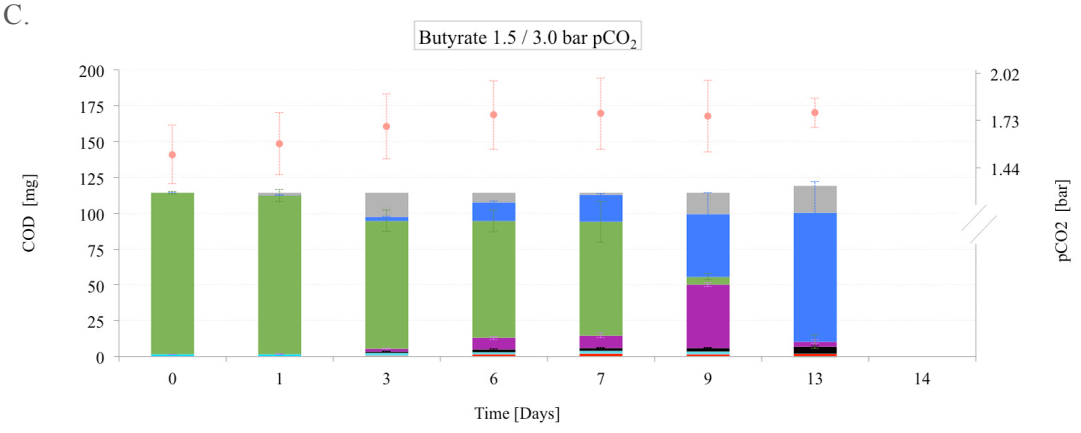
Butyrate 1.5 / 3.0 bar pCO2
COD [mg]
pCO2 [bar]
Time [Days]

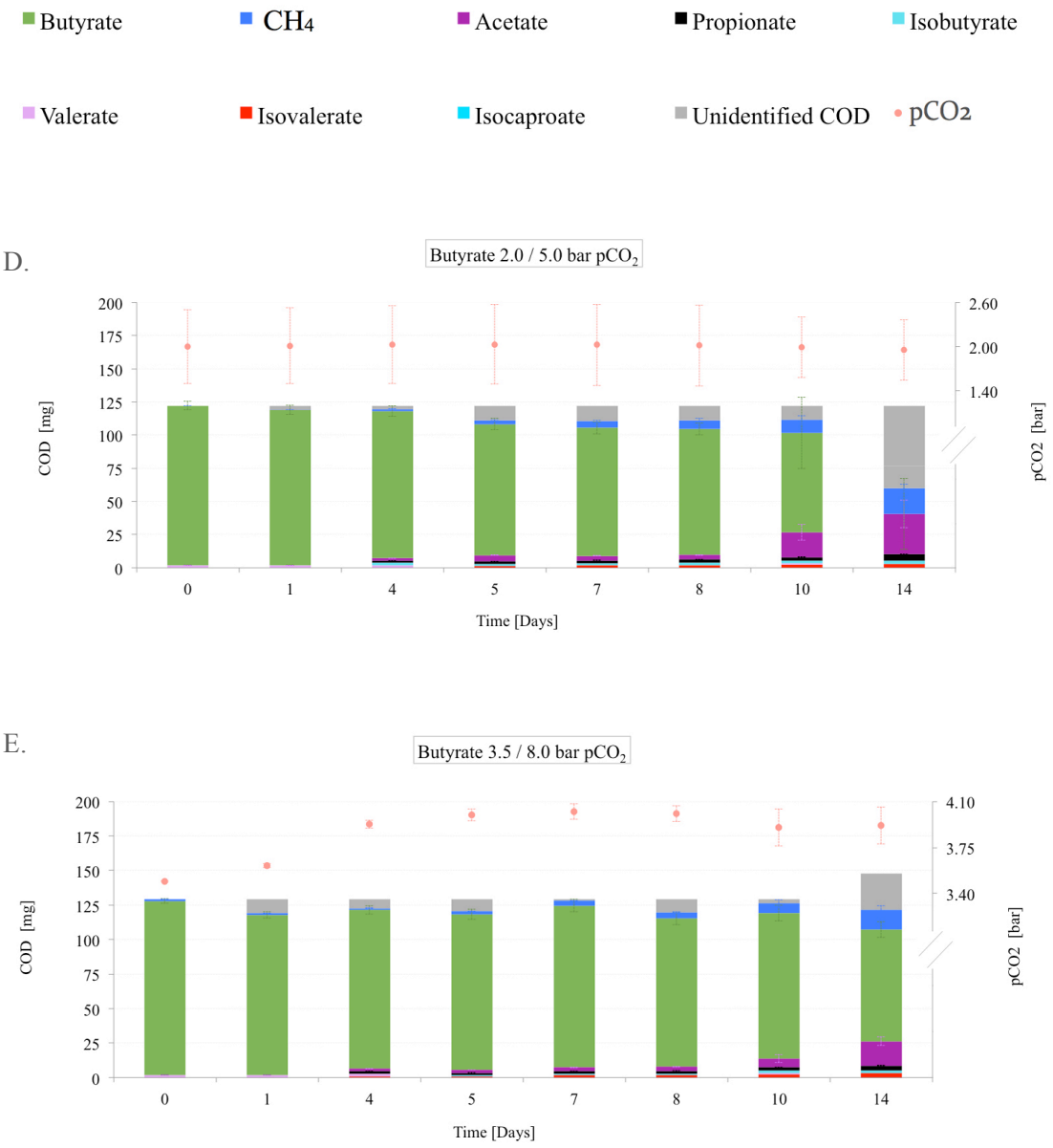

Figure 4-4. Product spectrum in the fermentative degradation of butyrate at 5 different CO_2 partial pressures: (A). 0.2 bar; (B). 1.0 bar; (C). 3.0 bar; (D). 5.0 bar; (E). 8.0 bar

As per the information provided in Figure 4-4, a proportion of the metabolites that were formed during the butyrate fermentation experiments, particularly at lower CO_2 partial pressures, could not be measured by gas chromatography (i.e. areas shaded in gray in Figure 4-4).

As a common metabolite and potential mechanism for energy conservation in the butyrate degradation pathway, as reported in the literature, it can be hypothesized that a proportion of this unidentified COD may correspond to formate [21]. This hypothesis has however not been confirmed as part of this investigation. Similarly, although not measured as part of this study, a proportion of this unidentified COD fraction may have been utilized for microbial growth, although biomass growth is expected to have been negligible at the experimental conditions tested (i.e. short duration batch tests with substrate concentrations below 13 mM).

Table 4-2 provides an overview of the relative abundance of the main electron sinks that were identified at the end of the butyrate experiments, for each of the CO_2 partial pressures tested. This information has also been depicted in Figure 4-5.

Table 4-2. Fractions of electron sinks at different pCO_2 conditions at the end of the butyrate degradation experiments

Compound	**Initial pCO_2 [pH]**				
	0.2 [6.9]	**1.0 [6.6]**	**3.0 [6.5]**	**5.0 [6.4]**	**8.0 [6.2]**
% CH_4	**42 ± 1.7**	**51 ± 2.0**	**74 ± 19**	16 ± 2.4	11 ± 2.0
% Acetate	1 ± 0.1	1 ± 0.3	3 ± 1.0	25 ± 8.5	14 ± 2.4
% Propionate	3 ± 0.3	3 ± 0.2	3 ± 0.4	2 ± 0.2	2 ± 0.2
% Isobutyrate	FD	FD	FD	2 ± 0.1	2 ± 0.1
% Valerate	FD	FD	-	FD	FD
% Isovalerate	1 ± 0.1	1 ± 0.1	2 ± 0.1	3 ± 0.2	3 ± 0.1
% Isocaproate	-	-	FD	-	-
% Residual butyrate	**FD**	**FD**	**FD**	**FD**	**47 ± 4.4**
% Unidentified COD (e.g. Formate, new biomass)	53 ± 5.8	44 ± 4.0	17 ± 6.3	50 ± 17	20 ± 3.8

**FD = Fully Degraded (This metabolite was fully degraded by the end of the experiment).*

**** Although H_2 was an additional intermediate electron sink formed via oxidation of butyrate into acetate and propionate, H_2 partial pressures remained below the GC's detection limit at all times for all of the experiments (< 60 Pa pH_2). H_2 was consumed effectively via the formation of methane in the butyrate experiments.*

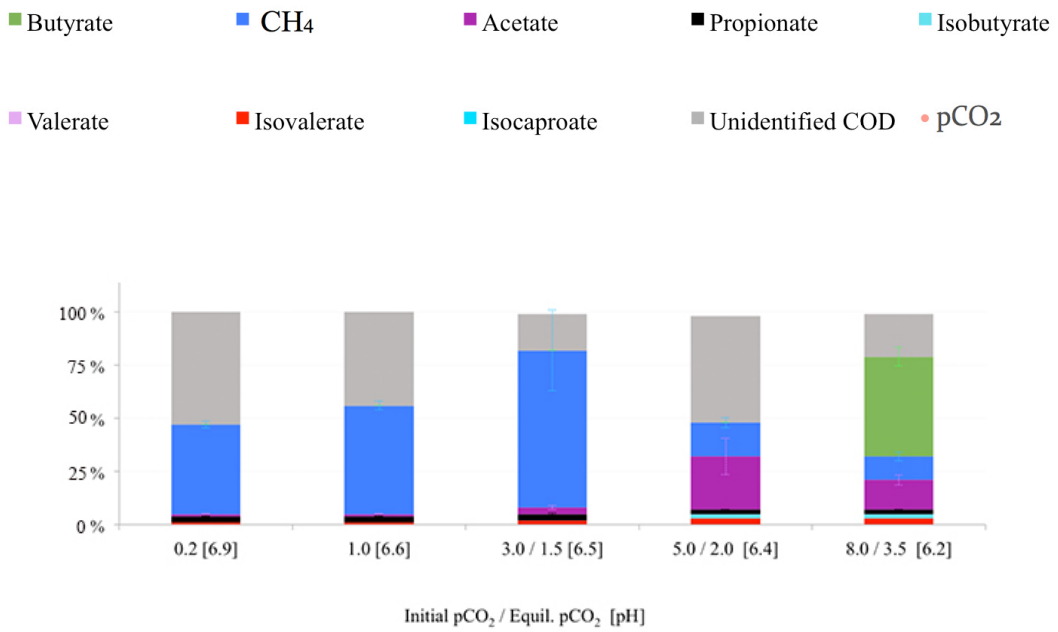

Figure 4-5. Overview of the product spectrums at 5 different CO_2 partial pressures at the end of the butyrate experiments

An assessment of the relative abundance of the range of metabolites that were measured by the end of the butyrate experiments, as presented in Figure 4-5, appears to indicate that elevated CO_2 partial pressures led to decreased butyrate degradation via either acetate and/or propionate formation. When considering that none of these butyrate oxidation routes involves any carboxylation step, it was expected that increasing availability of dissolve CO_2 in the reactors, with no route allowing consumption of this excess CO_2, would have a detrimental impact in the overall degradation of butyrate.

Additionally, increasingly higher pCO_2's appear to have correlated with the occurrence of a lag phase that led to incomplete butyrate degradation during the experiments conducted at 8.0 bar pCO_2 (i.e. 47 ± 4.4% of the Butyrate-COD fed at the start of the 8.0 bar pCO_2 experiments remained undegraded after 14 days of operation). Alternatively, and/or in addition to the potential detrimental effects of CO_2, limited butyrate degradation and the occurrence of a lag phase could have been related to toxicity based inhibition by elevated concentrations of undissociated butyrate in the reactors. In assessing this hypothesis, estimates of the concentrations of undissociated butyrate at the range of pH values of these experiments were calculated via Eq. 4-1 [66]. These calculations were based on the initial concentration of butyrate added to the reactors as substrate (i.e. 7 mM), the acid dissociation constant (pKa) for butyric acid of 4.83 and the pH in the reactors at different CO_2 partial pressures, as calculated in Section 3.3. An

overview of the undissociated butyrate concentrations at the range of pCO2 ‘s of these trials is presented in Table 4-3.

$$C_{UB} = \frac{C_{Total}}{1+10^{pH-pKa}}$$ Eq. 4-1

Where:

- C_{UB}: concentration of undissociated butyrate
- C_{Total}: initial concentration of butyrate as substrate (i.e. 7 mM)
- pKa: 4.83 for butyric acid

Table 4-3. Concentration of undissociated butyric acid in the butyrate degradation experiments at different pCO_2’s/pH

pH [Equil. pCO_2]	**Undissociated Butyrate [mM]**
6.9 [0.2]	0.06
6.6 [1.0]	0.12
6.5 [1.5]	0.15
6.4 [2.0]	0.18
6.2 [3.5]	0.29

As reported by van den Heuvel et al. [67], the critical inhibitory concentration of undissociated butyric acid is in the order of 50 mM. Other authors [68] indicate that inhibition or toxicity by undissociated butyric acid may arise when concentrations of this compound rise to approximately 13 mM. With an initial butyrate concentration of 7 mM and a minimum pH in the order of 6.2 for trials conducted at 8 bar pCO_2, the concentrations of undissociated butyrate estimated for the present set of experiments lay well below this toxic levels, at a maximum of approximately 0.3 mM. In this sense, it is believed that the limited butyrate degradation and the occurrence of a lag phase that were observed in this study may not be associated with toxicity due to elevated concentrations of undissociated butyrate but may be related to elevated CO_2 itself.

While the fermentative oxidation of butyrate was overall negatively impacted by elevated pCO_2's, provided some extent of butyrate degradation had already taken place and considering that H_2 was effectively consumed (H_2 partial pressures remained below the detection limit of 60 Pa) throughout the experiments, it is hypothesized that hydrogenotrophic methanogenesis was promoted by elevated pCO_2's. Considering that hydrogenotrophic methanogenesis is indeed a CO_2 consuming reaction, it is very plausible that higher CO_2 availability in the systems may have led to increased CH_4 formation from H_2 utilizing archaea.

The trend for increased CH_4 production by H_2 consuming methanogens at higher pCO_2's can be readily confirmed by evaluating the results from the 0.2 – 3.0 bar experiments, which indicate that final Methane-COD fractions increased from 42 ± 1.7% up to 74 ± 19% during these experiments, respectively. Although, as a result of a lag period of at least 3 days, the 5.0 and 8.0 bar pCO_2 experiments did not reach complete acetate and/or butyrate degradation and, consequently, do not necessarily reflect the trend for increased hydrogenotrophic methanogenesis at increasing pCO_2's, it is hypothesized that had these tests been allowed to run for a longer period of time, correspondingly higher fractions of CH_4 would have been observed from these experiments as well.

Following a similar trend to that reported for the pyruvate degradation experiments, with small amounts of propionate accumulating in the presence of all CO_2 partial pressures tested, further decarboxylation+oxidation of propionate into acetate appears to have been inhibited as a consequence of elevated pCO_2's in the reactors.

4.1.2.1. Main catabolic pathways in the fermentative degradation of butyrate

Based on the range of products that were identified over the course of the butyrate experiments, it is hypothesized that the major catabolic pathways that were involved in the anaerobic degradation of this substrate are as presented in Figure 4-6.

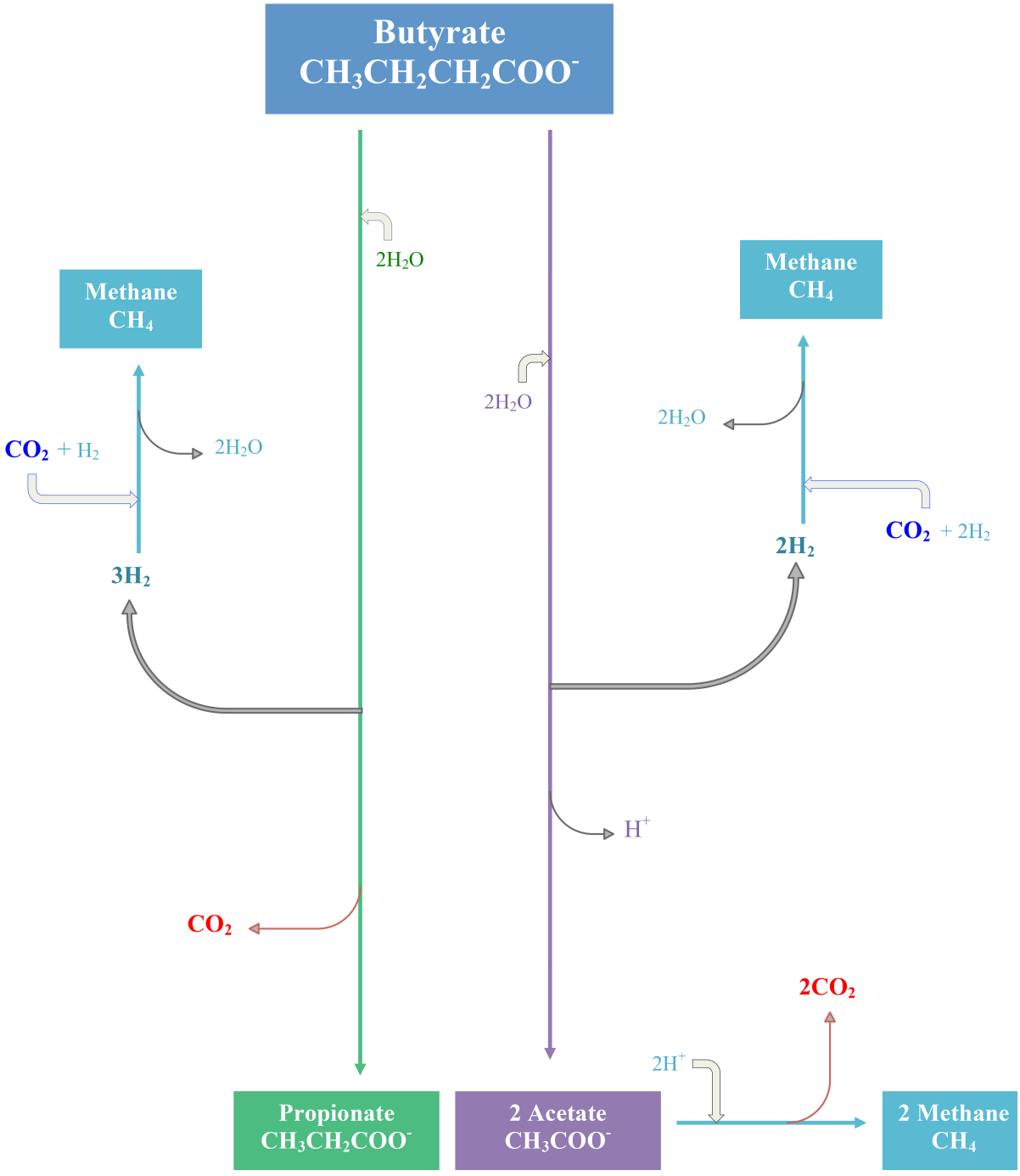

Figure 4-6. Major catabolic pathways involved in the anaerobic degradation of butyrate at varying CO_2 partial pressures

While the degradation of butyrate associated with the production of propionate involves a decarboxylation step (see Figure 4-6), it is interesting to note that butyrate degradation via acetate production neither involves CO_2 production nor CO_2 consumption directly. In this sense, elevated CO_2 partial pressures were expected to have a larger effect on the butyrate to propionate degradation pathway, while the butyrate to acetate degradation route was expected to remain relatively unchanged. From observation of Figure 4-4 however, both propionate and acetate formation from butyrate appear to have decreased with increasing pCO_2's, which suggests that excess dissolved CO_2 concentrations may have also impacted the metabolic activity of butyrate consuming bacteria at a more fundamental functional level, as opposed to only relating to end-product inhibition.

4.2. Thermodynamic Analyses

Following the preliminary identification of the product spectrums and the catabolic pathways involved in the pyruvate and butyrate degradation experiments, an assessment of the thermodynamic viability of the predominant reactions involved in these metabolic networks was conducted as part of this study. After the stoichiometries for each of the main reactions identified in the pyruvate and butyrate fermentation trials were determined, the $\Delta G^{0'}$ values, or the free energy changes at standard conditions and a pH of 7 (i.e. concentrations of aqueous species except H^+: 1 M, $[H^+] = 1x10^{-7}$ M, gaseous species: 1 atm, temperature 298.15 K) were calculated with Eq. 2-15 and Eq. 2-16 presented in Section 2.4. The G_f^0 (i.e. standard free energy of formation from the elements) used in Eq. 2-15 were sourced from tabulated values, as reported in the literature [65].

Subsequently, Gibbs free energy changes at actual conditions of temperature (i.e. 35°C), metabolite concentrations, gas partial pressures and pH, denoted as ΔG, were determined via Eq. 2-15 and Eq. 2-17, presented in Section 2.4. However, given the limitations associated with the impossibility to measure e.g. H_2 partial pressures below the detection limit of the equipment used in conducting this research (i.e. 60 Pa), as well as the difficulty of acquiring a highly accurate and complete dataset of all the intracellular metabolite concentrations that are also of relevance in conducting a precise quantification of reaction energetics in this study (e.g. succinate), most of the free energies calculated as part of this thesis work are *indicative values* only. While the calculation of the Gibbs free energy changes presented in this section and Tables A.1 through A.6 in Appendix A are based on the actual concentrations -as measured from these batch experiments- for most of the compounds that are involved in the fermentative degradation of pyruvate and butyrate, the concentrations of other relevant

metabolites used in estimating these ΔG values correspond to typical quantities that have been sourced from the literature. While the concentrations of the different metabolites varied in time, as each metabolite was either produced and/or consumed over the course of the trial, the concentrations that were used for the calculations of the ΔG values for each reaction correspond to those that would make each of these reactions as favorable as possible. That is, the concentrations at the specific moment in time with the highest concentrations of reactants and the lowest concentrations of products, as relevant for each individual reaction.

In the absence of a precise measurement for the actual H_2 partial pressure in the reactors, each of the Gibbs free energy calculations that have been undertaken in this study were performed using two different pH_2 values, namely at an minimum boundary value of $pH_2 = 1$ Pa, that corresponds to the average H_2 partial pressure in properly functioning anaerobic digestion applications [15], and a maximum boundary value of $pH_2 = 60$ Pa, corresponding to the detection limit of the equipment that was used in measuring the gas composition in the present experiments. In this sense, these calculations provide an indication of the range of plausible Gibbs free energy changes (i.e. maximum and minimum plausible energy yields, as dictated by the prevailing H_2 partial pressure) associated to each of the metabolic routes of pyruvate and butyrate fermentation that were considered as part of this study.

For reference, Table 4-4 provides a summary of the metabolite concentrations that have been used in these thermodynamic calculations, as well as information on the source of the data.

Table 4-4. Metabolite concentrations used in the thermodynamic calculations

Compound	Pyruvate Experiments	Butyrate Experiments	Data Source
Acetate [mM]	0.35 ± 0.1 (Rxn I and II) 0.12 ± 0.05 (Rxn IV) 1.50 ± 0.5 (Rxn V)	0.3 ± 0.05 (Rxn I) 3.4 ± 2.0 (Rxn IV)	Measured in this experiment (GC)
Propionate [mM]	0.13 ± 0.02 (Rxn II and IIIb) 2.00 ± 1.0 (Rxn IV)	0.12 ± 0.04	Measured in this experiment (GC)
Pyruvate [mM]	12.5 ± 1.6	-	Measured in this experiment (HPLC)
Butyrate [mM]	-	7.0 ± 1.5	Measured in this experiment (GC)
Succinate [mM]	1.0	-	Flamholz *et al*., 2012 [64]
pH_2 [bar]	1×10^{-5} (1 Pa) 6×10^{-4} (60 Pa)	1×10^{-5} (1 Pa) 6×10^{-4} (60 Pa)	Van Lier *et al*., 2008 [15] GC Detection Limit
Equil. pCO_2 [bar]	0.2, 1.0, 1.3, 1.9, 3.3	0.2, 1.0, 1.5, 2.0, 3.5	Measured in this experiment (manometer or pressure sensor + GC)
pCH_4 [bar]	0.02 ± 0.01	0.003 ± 0.002 (Rxn III) 0.06 ± 0.05 (Rxn IV)	Measured in this experiment (manometer or pressure sensor + GC)

Although, in light of these limitations, the thermodynamic quantities that are presented in this study are *indicative values*, they still provide an adequate base for inferring general trends that can *contribute* to elucidating the effects of elevated CO_2 partial pressures on the fermentative degradation of pyruvate and butyrate.

4.2.1. Energetics of pyruvate conversions

For the purpose of assessing the thermodynamic feasibility of the main metabolic routes in pyruvate fermentation, the stoichiometries of the overall reactions that were most predominantly observed in the pyruvate degradation experiments were defined and have been summarized in Table 4-5. The Gibbs free energy changes presented in this

table correspond to the free energy changes at standard conditions and a pH of 7 (i.e. concentrations of aqueous species except H^+: 1 M, $[H^+]$ = 1x10^{-7} M, gaseous species: 1 atm, temperature 298.15 K), denoted as $\Delta G^{0'}$, and were calculated with Eq. 2-15 and Eq. 2-16 in Section 2.4.

Table 4-5. Stoichiometries for the main reactions in the pyruvate degradation experiments

Reaction No.	Reaction Stoichiometry	$\Delta G^{\circ\prime}$ [kJ/reaction]
Fermentation/Acetogenesis		
I.	Pyruvate to Acetate $CH_3COCOO^- + H_2O \rightarrow CH_3COO^- + H_2 + CO_2$	-52.0
II.	Pyruvate to Acetate and Propionate $CH_3COCOO^- + \frac{1}{3} H_2O \rightarrow \frac{2}{3} CH_3COO^- + \frac{2}{3} CO_2 + \frac{1}{3} CH_3CH_2COO^-$	-75.9
IIIa.	Pyruvate to Succinate $CH_3COCOO^- + 2H_2 + CO_2 \rightarrow {}^-OOCCH_2CH_2COO^- + H_2O + H^+$	-98.4
IIIb.	Succinate to Propionate $^-OOCCH_2CH_2COO^- + H^+ \rightarrow CH_3CH_2COO^- + CO_2$	-25.3
IV.	Propionate to Acetate $CH_3CH_2COO^- + 2H_2O \rightarrow CH_3COO^- + 3H_2 + CO_2$	+71.7
Methanogenesis		
V.	Acetate to Methane $CH_3COO^- + H^+ \rightarrow CH_4 + CO_2$	-35.7

Based on these reaction stoichiometries, the operating temperature of 35°C and the concentrations for reactants and products as provided in Table 4-4, the corresponding Gibbs free energy changes (ΔG) for these biochemical conversions have been determined for the range of CO_2 partial pressures and corresponding equilibrium pH's evaluated as part of this research. As per the example calculation provided in Appendix A and the supplementary Excel® spreadsheet that has been provided with this document, these ΔG values have been determined via Eq. 2-15 and Eq. 2-17 in Section 2.4.

Figure 4-7 below provides a graphical depiction of these Gibbs free energy changes (ΔG), as calculated for each of the reactions presented in Table 4-5, against the equilibrium CO_2 partial pressures and corresponding pH values examined in this study. Note that these figures provide plausible maximum and minimum energy yields for each reaction, as calculated using assumed boundary values for the H_2 partial pressure of 1 Pa (red markers) and 60 Pa (blue markers).

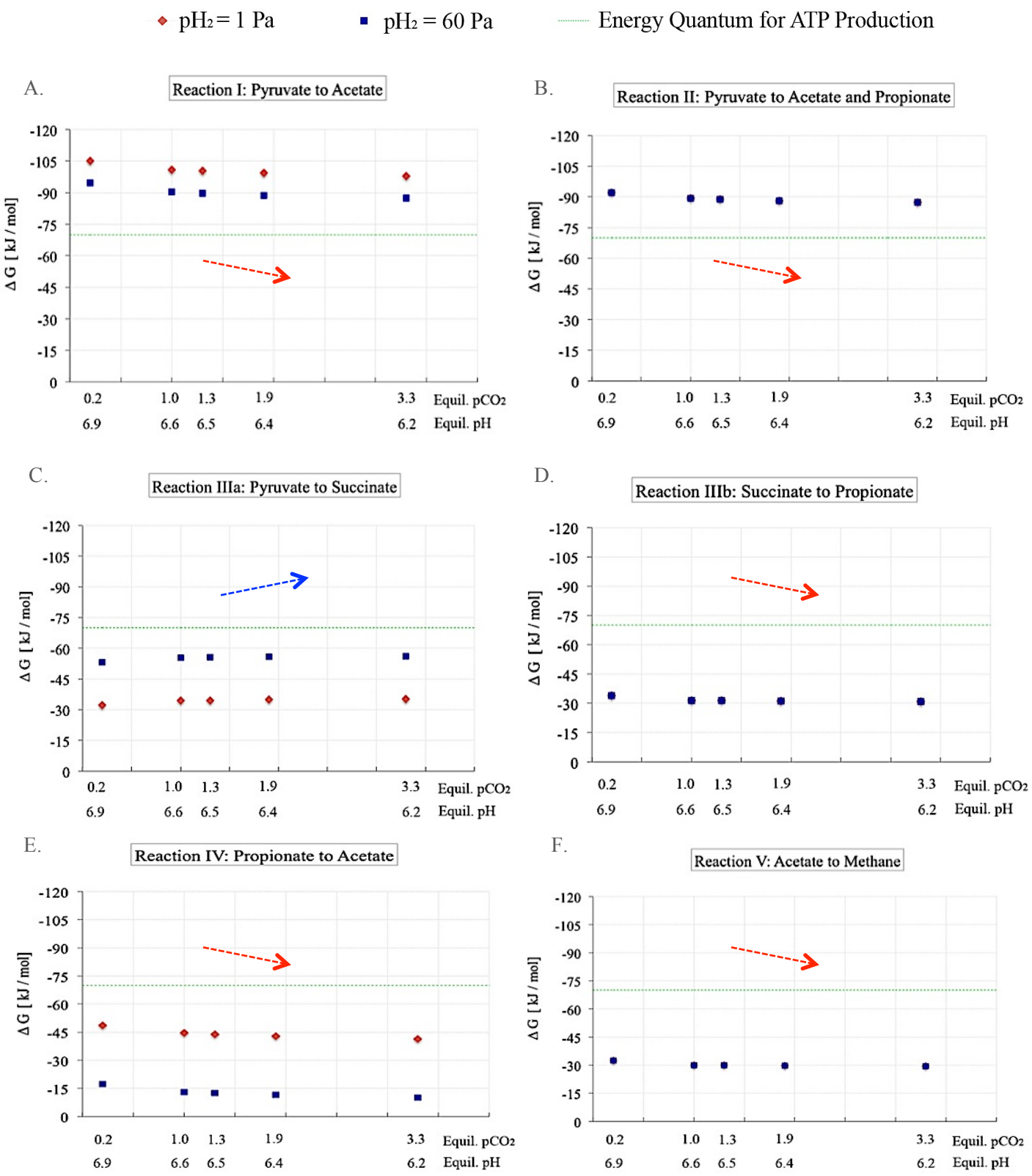

Figure 4-7. Effect of increasing pCO_2's on the energy yields for the main catabolic reactions in pyruvate fermentation: (A). Reaction I: Pyruvate to Acetate; (B). Reaction II: Pyruvate to Acetate and Propionate; (C). Reaction IIIa: Pyruvate to Succinate; (D). Reaction IIIb: Succinate to Propionate; (E). Reaction IV: Propionate to Acetate; (F). Reaction V: Acetate to Methane.

As indicated by the arrows in Figure 4-7, most of the energy yields associated with the fermentation routes of pyruvate, as observed in this study, followed a downward trend in response to increasingly higher CO_2 partial pressures. As expected, it can be observed that the trend for less negative ΔG values at elevated pCO_2's coincided with decarboxylation/CO_2 releasing reactions (i.e. conversion of pyruvate to acetate, succinate to propionate, propionate to acetate and acetate to methane). On the other hand, the reductive step from pyruvate to succinate, which corresponds to a carboxylation/CO_2 consuming reaction, evidenced a trend for higher energy yields at increasingly higher CO_2 partial pressures.

With indicative ΔG values ranging between approximately -105 kJ/mol and -88 kJ/mol at all pCO_2 conditions tested and pH_2's of between 1 and 60 Pa, the conversion of pyruvate into acetate was the most thermodynamically favorable reaction in the pyruvate fermentation experiments. Additionally, considering that the quantum of energy that is needed for the synthesis of 1 mol of ATP is approximately -70 kJ.mol-ATP^{-1} [30] (i.e. indicated by the green lines in Figure 4-7), the oxidation + decarboxylation of pyruvate into acetate was the only ATP yielding conversion, synthesizing approximately 1 mol-ATP.mol-$Acetate^{-1}$. As presented in Figure 4-7, although all other reactions were exergonic at the conditions of these experiments and assumed H_2 partial pressures of between 1 and 60 Pa, their energy yields were lower with indicative ΔG values ranging between -60 and -10 kJ/mol.

With acetate, propionate and methane as the main metabolites/end products observed during the pyruvate degradation experiments (see Figure 4-1), it was expected that the metabolic routes leading to these products were to be exergonic at the experimental conditions tested, as confirmed by the outputs of the indicative thermodynamic analyses conducted in this study.

With the apparent accumulation of propionate at pCO_2's above 3 bar, as observed in Figure 4-2, it appears that the oxidation of propionate into acetate was somewhat inhibited at these higher CO_2 partial pressures. While a complete analysis of the influence of elevated CO_2 partial pressures on the degradation of propionate was out of the scope of this study, it is interesting to observe that, in comparison to the ΔG values calculated at a H_2 partial pressure of 1 Pa (i.e. between -49 and -42 kJ/mol), the ΔG estimates at relatively high H_2 partial pressures of 60 Pa (i.e. between -17 to -10 kJ/mol) indicate that this conversion is highly sensitive to the prevailing H_2 partial pressure in the system. Assuming that the H_2 partial pressure in the reactors was close to the equipment's detection limit of 60 Pa, it is plausible that one of the factors leading to propionate accumulation may be related to the energetic limitations associated with potentially high H_2 partial pressures in the reactors (i.e. in the vicinity of 60 Pa).

4.2.2. Energetics of butyrate conversions

For the purpose of assessing the thermodynamic feasibility of the main metabolic routes in butyrate fermentation, the stoichiometries of the overall reactions that were most predominantly observed in the butyrate degradation experiments were defined and have been summarized in Table 4-6. The Gibbs free energy changes presented in this table correspond to the free energy changes at standard conditions and a pH of 7 (i.e. concentrations of aqueous species except H^+: 1 M, $[H^+]$ = 1x10^{-7} M, gaseous species: 1 atm, temperature 298.15 K), denoted as $\Delta G^{0'}$, and were calculated with Eq. 2-15 and Eq. 2-16 in Section 2.4.

Table 4-6. Stoichiometries for the main reactions in the butyrate degradation experiments

Reaction No.	Reaction Stoichiometry	$\Delta G^{\circ\prime}$ [kJ/reaction]
Fermentation/Acetogenesis		
I.	Butyrate to Acetate $CH_3CH_2CH_2COO^- + 2H_2O \rightarrow 2CH_3COO^- + H^+ + 2H_2$	+48.1
II.	Butyrate to Propionate $CH_3CH_2CH_2COO^- + 2H_2O \rightarrow CH_3CH_2COO^- + CO_2 + 3H_2$	+71.5
Methanogenesis		
III.	Hydrogen to Methane $4H_2 + CO_2 \rightarrow CH_4 + 2H_2O$	-130.7
IV.	Acetate to Methane $CH_3COO^- + H^+ \rightarrow CH_4 + CO_2$	-35.7

Based on these reaction stoichiometries, the operating temperature of 35°C and the concentrations for reactants and products as provided in Table 4-4, the corresponding Gibbs free energy changes (ΔG) for these biochemical conversions have been determined for the range of CO_2 partial pressures and corresponding equilibrium pH's evaluated as part of this research. As per the example calculation provided in Appendix A and the supplementary Excel® spreadsheet that has been provided with this document, these ΔG values have been determined via Eq. 2-15 and Eq. 2-17 in Section 2.4.

Figure 4-8 below provides a graphical depiction of these Gibbs free energy changes (ΔG), as calculated for each of the reactions presented in Table 4-6, against the equilibrium CO_2 partial pressures and corresponding pH values examined in this study. Note that these figures provide plausible maximum and minimum energy yields for each reaction, as calculated using assumed boundary values for the H_2 partial pressure of 1 Pa (red markers) and 60 Pa (blue markers).

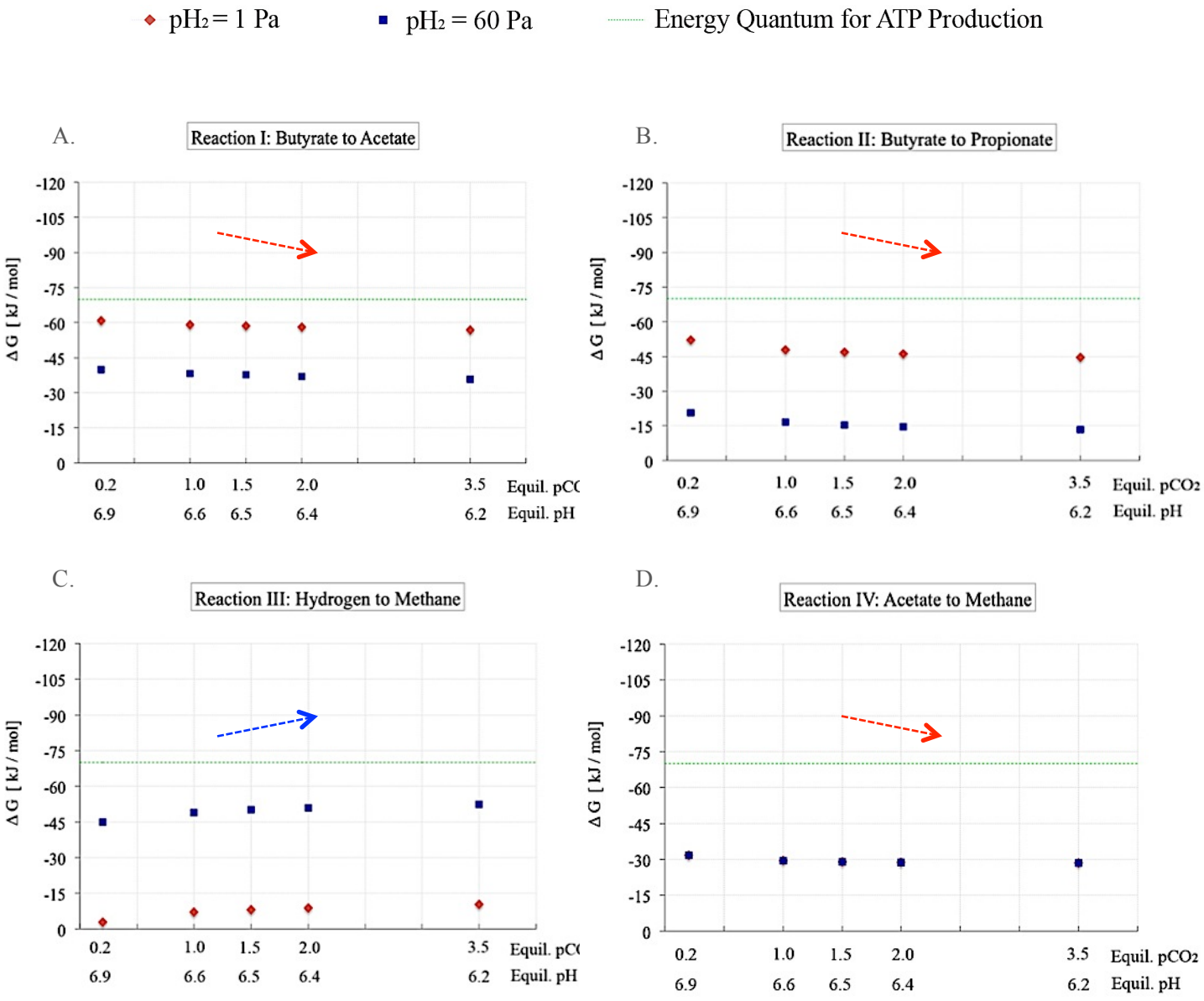

Figure 4-8. Effect of increasing pCO_2's on the energy yields for the main catabolic reactions in butyrate fermentation: (A). Reaction I: Butyrate to Acetate; (B). Reaction II: Butyrate to Propionate; (C). Reaction III: Hydrogen to Methane; (D). Reaction IV: Acetate to Methane.

According to the indicative range of ΔG values for the different metabolic routes of butyrate, as provided in Figure 4-8, with the exception of the CO_2 consuming conversion of H_2 into methane by hydrogenotrophic archae, the energy yields associated with the metabolic routes of butyrate, as observed in this study, followed a downward trend in response to increasingly higher CO_2 partial pressures (as indicated by the arrows in Figure 4-8). Additionally, from evaluation of the changes in the energy yields estimated at the boundary pH_2 values of 1 Pa and 60 Pa, it appears evident that butyrate degradation via either acetate and/or propionate formation is strongly dependent on the prevailing H_2 concentrations in the systems.

While the oxidation of butyrate into acetate was the most thermodynamically favorable reaction at all the pCO_2's conditions tested (i.e. indicative Gibbs free energy changes ranging between -61 kJ/mol and -36 kJ/mol at pCO_2's of between 0.2 and 8 bar and H_2 partial pressures of between 1 and 60 Pa), the energy yields from the conversion of butyrate into acetate also followed a downward trend with increasing pCO_2's. Although CO_2 is neither a substrate nor a product in the oxidative fermentation of butyrate into acetate, and thus the detrimental effects of elevated pCO_2's on the energetics of this metabolic pathway may not be readily discernible, increasingly higher CO_2 partial pressures led to a corresponding decrease in the operating pH's, as determined in Section 3.3. In this sense, while the pH of the 0.2 bar pCO_2 experiments was estimated at 6.9, operating at elevated CO_2 partial pressures led to a substantial pH drop, with a pH of 6.2 estimated for the 8.0 bar pCO_2 trials. Considering H^+ ions are a by-product in the conversion of butyrate into acetate and H_2, it is hypothesized that lower energetic yields at higher CO_2 partial pressures were the result of increasingly high concentrations of H^+ ions in the liquid broth, which were associated to the lower pH values at increasing pCO_2's.

Similarly, the indicative energy yields associated with the degradation of butyrate into propionate appeared less negative in response to elevated CO_2 partial pressures, with indicative energy yields decreasing from -52 kJ/mol to -45 kJ/mol and from -21 kJ/mol to -13 kJ/mol between 0.2 and 8.0 bar pCO_2's at the assumed boundary H_2 partial pressures of 1 Pa and 60 Pa, respectively. This trend for lower energy yields at increasing pCO_2's is however not unexpected in this metabolic route, considering that the oxidation of butyrate into propionate corresponds to a decarboxylation step, with CO_2 being released during this conversion, as depicted in Figure 4-6.

With acetate, propionate and methane as the main metabolites/end products observed during the butyrate degradation experiments (see Figure 4-4), it was expected that the metabolic routes leading to these products were to be exergonic at the experimental conditions tested, as confirmed by the outputs of the indicative thermodynamic analyses conducted in this study.

However, according to Figure 4-8, and in comparison to the results from the fermentative degradation of pyruvate (Figure 4-7), it appears that the biochemical conversions that took place in the butyrate fermentation experiments proceeded at much more limited energy yields (i.e. closer to thermodynamic equilibrium). In particular, it can be observed that none of these reactions appeared to have yielded sufficient energy for effective synthesis of ATP (i.e. ΔG values were below the energy quantum for synthesis of 1 mol of ATP of -70 kJ for all conversions). Thus, although all reactions appeared exergonic at the conditions of these experiments, their energy yields were relatively low at ΔG values ranging between a potential maximum of -60 kJ/mol and a potential minimum of -3 kJ/mol.

As reported in the literature [29], a consequence of operating in close proximity to this thermodynamic boundary condition is that these conversions may proceed at very low conversion rates. Thus, the occurrence of a lag phase during the butyrate degradation experiments, which was particularly noticeable at elevated pCO_2's above 3.0 bar, may have been linked to these energetic limitations.

4.3. Kinetic Analyses

In addition to the effects of varying pCO_2's on the thermodynamic viability of the main metabolic pathways in the pyruvate and butyrate degradation experiments, elevated CO_2 partial pressures appear to have had an impact on the conversion rates of pyruvate, butyrate and/or the main intermediate metabolites that were formed during these anaerobic conversions, as discussed in Sections 4.3.1 and 4.3.2 below.

In performing these kinetic analyses, all degradation and/or production rates have been estimated by means of linear regressions that were fitted to observed data on the evolution of the substrate/metabolite concentrations over time, as measured from the experiments. While the information that was derived from these linear model fittings allowed an assessment of the general variations in these conversion rates in response to increasing CO_2 partial pressures, it is important to note that these linear models are unable to precisely incorporate the effects of lag phases and/or the effects of simultaneous production and consumption of metabolites, which may be better represented by non-linear fitting models (e.g. a Gompertz function). In light of these limitations, the conversion rates that have been determined as part of this investigation correspond to indicative, apparent consumption/production rates only.

4.3.1. Conversion rates in pyruvate fermentation

As a first step to estimating the indicative rates of conversion for the main metabolites in the pyruvate degradation experiments at different CO_2 partial pressures, the average concentrations of pyruvate, acetate and propionate, as measures from the batch experiments, were plotted against time and are as presented in Figure 4-9.

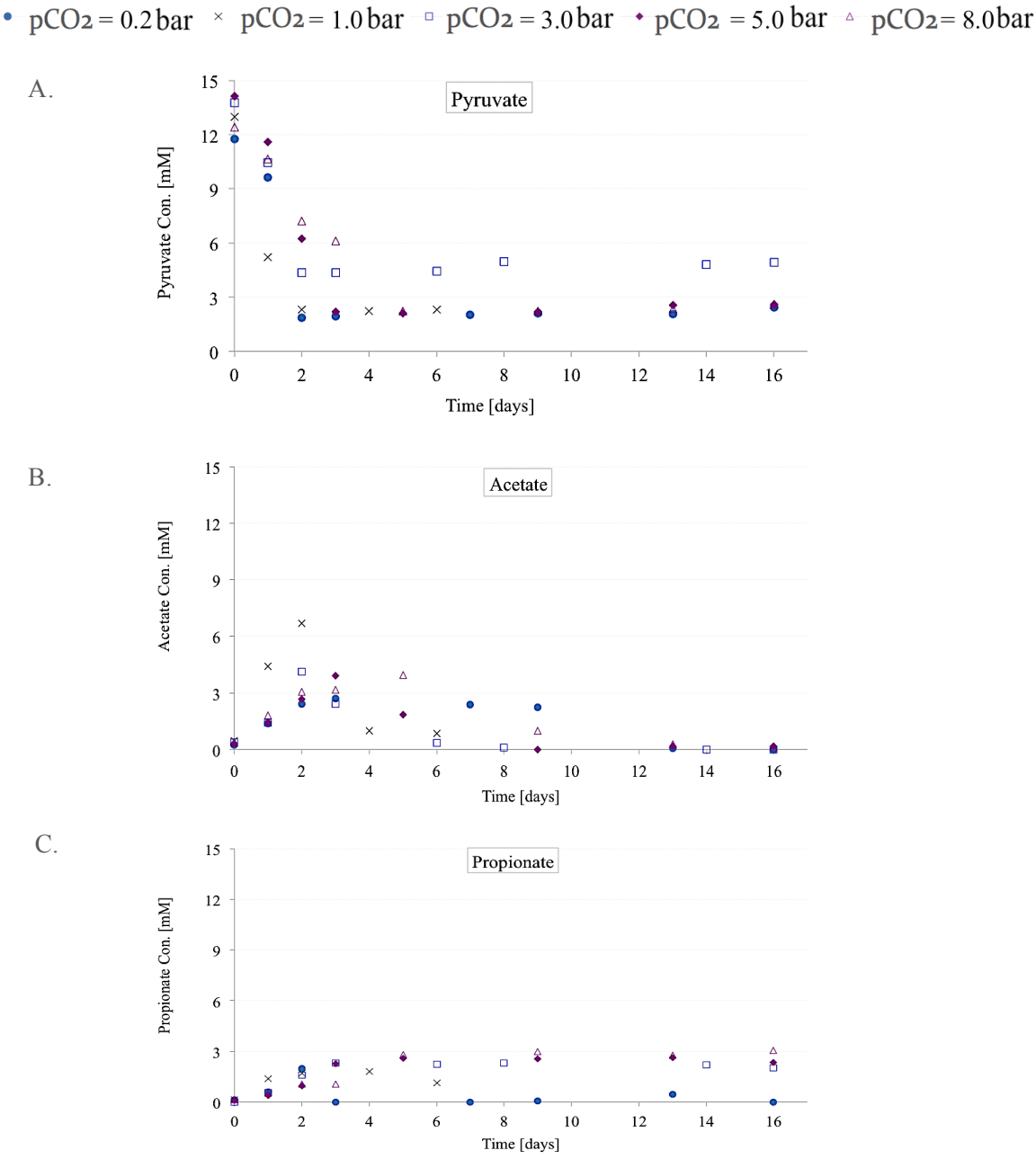

Figure 4-9. Changes in the concentrations of the main metabolites in the pyruvate experiments over time: (A). Pyruvate (B). Acetate and (C). Propionate

From observation of Figure 4-9, while changes in the concentrations of pyruvate and propionate followed a more or less discernable trend over the course of the experiments, identification of the patterns associated with variations in the concentration of acetate were less clear, in response to the occurrence of simultaneous production and consumption of this metabolite (i.e. further conversion of acetate into methane).

Table 4-7 and Table 4-8 below provide an overview of the indicative degradation rates for pyruvate and propionate that were determined via these linear fittings at the different set of pCO_2's conditions examined in this investigation.

Table 4-7. Indicative degradation rates for pyruvate at different CO_2 partial pressures

Initial pCO_2 / [Equil. pCO_2]	**Pyruvate Degradation Rate [mg $.l^{-1}.d^{-1}$]**	**% Reduction**
0.2 / [0.2]	435	-
1.0 / [1.0]	468	-
3.0 / [1.3]	413	5.0
5.0 / [1.9]	362	17.0
8.0 / [3.3]	181	58.0

Table 4-8. Indicative degradation rates for propionate at different CO_2 partial pressures

Initial pCO_2 / [Equil. pCO_2]	**Propionate Oxidation Rate [mg $.l^{-1}.d^{-1}$]**	**% Reduction**
0.2 / [0.2]	145	-
1.0 / [1.0]	24	83.0
3.0 / [1.3]	1.2	99.1
5.0 / [1.9]	1.16	99.2
8.0 / [3.3]	0.4	99.7

The estimates of the apparent degradation rates for pyruvate that were observed in these experiments indicate that increasingly high CO_2 partial pressures correlated with a decrease in the rates of pyruvate conversion. In particular, while the consumption rate

for pyruvate was estimated at approximately 435 mg Pyruvate.l^{-1}.d^{-1} when operating at a pCO_2 of 0.2 bar, the indicative degradation rate of this substrate was determined as approximately 181 mg Pyruvate.l^{-1}.d^{-1} for the 8.0 bar pCO_2 trials. Thus, with an indicative decrease in the pyruvate degradation rate of up to -58% when shifting the operating pCO_2 from 0,2 to 8.0 bar, it appears that elevated CO_2 availability in the system may have led to a certain extent of inhibition of the activity of (-potentially) rate limiting enzymes that catalyze pyruvate carboxylation and/or pyruvate decarboxylation (i.e. pyruvate carboxylase and/or the enzymes from the pyruvate dehydrogenase complex, respectively). However, with no formal measurements or analyses on the activities of specific enzymes conducted as part of this study, any potential influence of elevated CO_2 partial pressures on the activity of these catalysts could not be established.

Similarly, with an indicative decrease in the rate of propionate degradation of approximately -99%, when comparing the degradation rates for propionate at a pCO_2 of 0.2 bar (i.e. 145 mg Propionate.l^{-1}.d^{-1}) against this rate at 8.0 bar pCO_2 (i.e. < 1 mg Propionate.l^{-1}.d^{-1}), it is plausible that excess CO_2 availability may have had an impact on the enzymatic activity of e.g. propionate CoA-transferase, a key enzyme catalyzing the conversion of propionate into acetate. However, with no formal measurements or analyses on the activities of specific enzymes conducted as part of this study, any potential influence of elevated CO_2 partial pressures on the activity of these catalysts could not be established.

In this sense, although the identification of the specific mechanistic drivers behind the apparent detrimental effects of elevated CO_2 partial pressures on the rates of conversion of pyruvate and/or propionate were out of the scope of this study, it appears that one of the mechanisms leading to e.g. propionate accumulation in the reactors may have been related to the kinetic limitations of this reaction, which may have been linked to elevated CO_2 partial pressures.

4.3.2. Conversion rates in butyrate fermentation

As a first step to understanding the rates of conversion of substrates and metabolites taking place in the butyrate fermentation experiments, changes in the concentrations of butyrate, acetate and propionate were plotted against time and are presented in Figure 4-10.

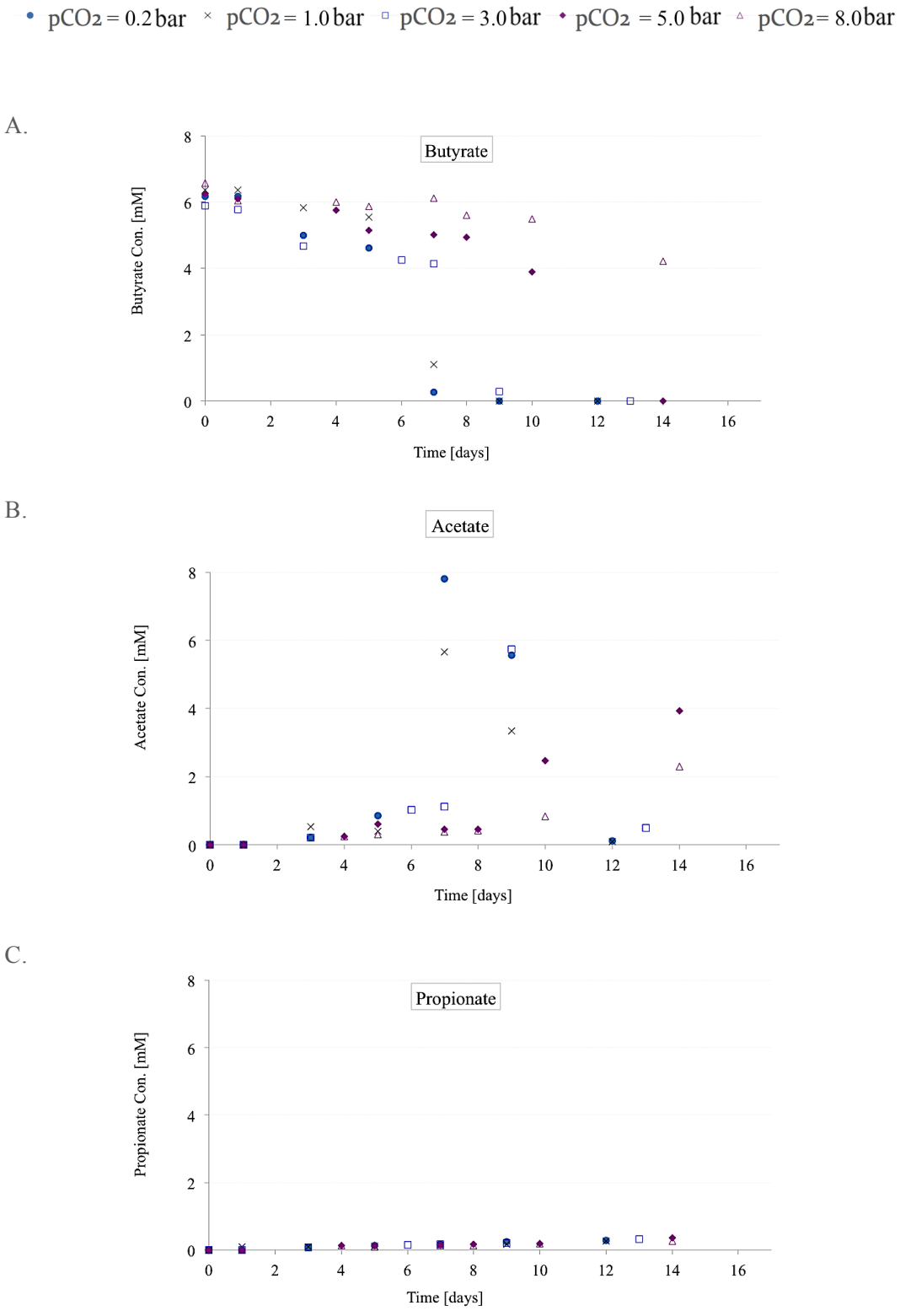

Figure 4-10. Changes in the concentration of the main metabolites in the butyrate experiments over time: (A). Butyrate, (B). Acetate and (C). Propionate

From inspection of these graphs, and in correspondence with the outputs from the pyruvate degradation experiments, while changes in the concentrations of butyrate followed a more or less discernable trend, identification of a clear pattern for changes in the concentration of acetate over the course of the experiments was unfeasible due to the occurrence of simultaneous production and consumption of this metabolite (i.e. further conversion of acetate into methane). Similarly, with very limited amounts of propionate produced during the butyrate degradation tests, as well as the occurrence of a lag phase during the experiments conducted at 3.0, 5.0 and 8.0 bar pCO_2, changes in the concentration of propionate over time could not be effectively fitted via the linear regression model used in this study.

Table 4-9 below provides a summary of the indicative butyrate degradation rates that were estimated for each of the pCO_2 conditions tested.

Table 4-9. Indicative rates for butyrate degradation at different CO_2 partial pressures

Initial pCO_2 / [Equil. pCO_2]	**Butyrate Degradation Rate [mg $.l^{-1}.d^{-1}$]**	**% Reduction**
0.2 / [0.2]	86	-
1.0 / [1.0]	70	19
3.0 / [1.5]	54	37
5.0 / [2.0]	39	55
8.0 / [3.5]	15	83

According to these indicative degradation rates for butyrate, it can be observed that increasingly high CO_2 partial pressures correlated with an apparent reduction in the conversion rates for this substrate, with rates decreasing from 86 mg Butyrate.$l^{-1}.d^{-1}$ at a pCO_2 of 0.2 bar down to approximately 15 mg Butyrate.$l^{-1}.d^{-1}$ when operating at 8 bar pCO_2, which corresponds to a decline in this conversion rate in excess of -80%.

Based on this outcome, it is plausible that certain key enzymes that are associated with the fermentative degradation of butyrate may have been inhibited in response to the harsh environmental conditions associated to increasingly high pCO_2's. Because these enzymes are catalysts that effectively decrease the activation energy (E_A) required for butyrate oxidation, with potentially higher activations energies and presumably limited energy availability, as per the thermodynamic analysis presented in Section 4.2.2., a decrease in the rate of butyrate consumption may have been related to such lower

enzymatic activities. As such, it is hypothesized that the microbial consortium that was involved in the fermentative degradation of butyrate had to undergo continuous adaptation to the prevailing environmental conditions in the reactors, which may explain, to a certain extent, the occurrence of a lag phase, as evidenced during the trials at 3.0, 5.0 and 8.0 bar pCO_2. However, with no formal measurements or analyses on the activities of specific enzymes conducted as part of this study, any potential influence of elevated CO_2 partial pressures on the activity of these catalysts could not be established.

Although the identification of the specific mechanistic drivers behind the apparent detrimental effects of elevated CO_2 partial pressures on the rates of conversion of butyrate were out of the scope of this study, it appears that one of the mechanisms leading to e.g. the occurrence of a lag phase in the butyrate degradation experiments may have been related to these kinetic limitations, which may have been linked to elevated CO_2 partial pressures.

5. GENERAL DISCUSSION AND CONCLUSIONS

In light of the outcomes of the present thesis work, it is proposed that exerting control over the operating CO_2 partial pressures can have a distinct effect in regulating the product spectrum in pyruvate and butyrate fermentation systems. In this sense, these findings tend to support the potential role of elevated pCO_2's as one control mechanism for targeted production of organic acids from the carboxylic platform that is worthwhile exploring further.

As the subject matter of this thesis, it was shown that both the faith of pyruvate and butyrate fermentations, two intermediate metabolites that are relevant in the anaerobic degradation of a range of complex organic compounds -including glucose, can be influenced via increasingly high operational CO_2 partial pressures.

In accordance to Henry's Law, a direct result of operating at pressurized CO_2 conditions was a certain extent of acidification of the liquid broth, via an increased migration of CO_2 from the gas phase and the formation of carbonic acid and increased concentration of weak acids in the liquid phase. Specifically, in the presence of a buffering capacity of 100 mM $NaHCO_3$, operating at CO_2 partial pressures of between 0.2 and 8.0 bar led to a drop in the pH from 6.9 to approximately 6.2, respectively. Although the activity of methanogenic archaea is susceptible to pH conditions below neutrality, substantial amounts of CH_4 were however still observed across all pCO_2's conditions tested, including at pH's of 6.2 (i.e. 8.0 bar pCO_2).

In relation to the pyruvate fermentation experiments, increasingly higher operating CO_2 partial pressures did however correlate with reduced acetate and CH_4 formation, while simultaneously leading to more propionate production and accumulation. In this sense, the outputs from these experiments suggest that while the main metabolic pathways that involve decarboxylation reactions (i.e. conversion of pyruvate into acetate, acetate into methane and propionate into acetate) were hindered at elevated pCO_2's, the pyruvate degradation routes that include a carboxylation step were promoted in the presence of higher availability of CO_2 in the reactors (i.e. conversion of pyruvate into propionate via succinate). Also in line with these findings, as a fermentative route that proceeds via a decarboxylation step, while butyrate was absent at elevated pCO_2's above 3.0 bar, limited amounts of butyrate (i.e. less than 2% of the Pyruvate-COD that was fed to the reactors) was formed at pCO_2's of 0.2 and 1.0 bar. Considering that the main metabolic route for synthesis of reducing power and ATP in the fermentative degradation of pyruvate corresponds to the oxidation of pyruvate into acetate, the reduction of pyruvate into propionate and/or butyrate was thus coupled to acetate formation in all cases.

In agreement with the findings from the pyruvate batch trials, the outcomes from the butyrate degradation experiments also suggest that higher CO_2 availability in the reactors hindered the formation of metabolites that are the result of decarboxylation steps. In the specific case of butyrate fermentation, this corresponded to a decrease in the formation of propionate from butyrate at increasingly higher pCO_2's. While the oxidation of butyrate into acetate is not directly linked to CO_2 consumption nor release, the outcomes from this study indicate that acetate formation appeared less favorable at elevated pCO_2's. The impact of CO_2 on this particular metabolic pathway appears more evident when considering that the oxidation of butyrate into acetate leads to the release of H^+ ions, and is thus sensitive to excess H^+ concentrations in the liquid broth. Because increasingly higher CO_2 dissolution led to a drop in the pH from 6.9 down to a minimum of 6.2 during the 8.0 bar pCO_2 experiments, higher concentrations of H^+ were present at increasing pCO_2 conditions and were thus detrimental for the conversion of butyrate into acetate. On the other hand, as a CO_2 consuming conversion, the production of CH_4 by hydrogenotrophic archaea was favored at elevated pCO_2's, as evidenced from increased methane formation in the butyrate experiments at increasingly higher pCO_2's up to 3.0 bar.

The observations on the role of elevated CO_2 partial pressures as a potential mechanism to steer product formation in the fermentation of pyruvate and butyrate were supported by the outcomes of the indicative thermodynamic and kinetic analyses conducted in this study. In general, indicative thermodynamic calculations -based on assumed pH_2's of between 1 and 60 Pa- suggest that increasing CO_2 partial pressures led to a trend for increasing energy yields for the conversions of pyruvate into propionate -via succinate- and H_2 into CH_4, both of which are CO_2 consuming routes. On the other hand, while all main pathways remained exergonic at the conditions of these experiments, fermentation of pyruvate via acetate and methane and of butyrate via propionate (i.e. CO_2 releasing reactions) appeared less thermodynamically viable in response to increasing pCO_2's.

Similarly, indicative calculations of the Gibbs free energy changes for the conversion of propionate into acetate, which may be a relevant step for both the fermentative degradation of pyruvate and butyrate, indicated that this conversion tended to become less energetically favorable at increasing pCO_2's. Additionally, the thermodynamic viability of the conversion of propionate into acetate was shown to be highly sensitive to the prevailing H_2 partial pressures in the reactors, which, in the absence of a precise measurement available for these experiments, could have laid anywhere between 1 and 60 Pa. According to the indicative thermodynamic calculations, in the event that the actual H_2 partial pressures in the reactors were just below the GC's detection limit of 60 Pa, the oxidation of propionate into acetate was highly energetically limited (i.e. energy yields decreasing from -17 kJ/mol to -10 kJ/mol in response to changes in the CO_2 partial pressure from 0.2 to 8.0 bar). Similarly, the degradation of butyrate via

acetate and/or propionate was shown to be energetically limited at elevated pCO_2's; these energy yields were also very sensitive to H_2 partial pressures. In particular, in the event the actual pH_2 in the reactors was in the order of 60 Pa, the indicative Gibbs free energy changes calculated for the conversion of butyrate into propionate indicated a decrease from -20 kJ/mol down to -13 kJ/mol in response to an increase in the pCO_2's from 0.2 to 8.0 bar. With H_2 partial pressures potentially in the order of 60 Pa, it is plausible that interspecies hydrogen transfer between the H_2 producing and the H_2 consuming microorganisms that were present in the mixed culture (e.g. acetogens and hydrogenotrophic methanogens) was not effectively achieved s a consequence of e.g. the flocculent/disaggregated nature of the inoculum. In turn, it is plausible that these low energy yields may have not been sufficient to support the metabolic requirements of either the propionate degrading or the butyrate fermenting bacteria in the mixed culture, thus leading to the accumulation of propionate in the pyruvate degradation experiments and the occurrence of a lag phase and limited degradation of butyrate in the butyrate fermentation trials.

According to the indicative analysis on the kinetics of pyruvate and butyrate degradation, increasing CO_2 partial pressures correlated with a decrease in these conversion rates by more than -50% and -80% when operating at a pCO_2 of 8.0 bar. It is plausible that this substantial decrease in the overall degradation rates of both pyruvate and butyrate be associated with inhibition of potentially rate limiting enzymes that are associated with the fermentation of these metabolites, as a response to the harsh environmental conditions associated to increasingly high pCO_2's.

BIBLIOGRAPHY

1. Cooper, A.J., Ginos, J.Z., Meister, A., 1983. Synthesis and properties of the a-keto acids. Chem. Rev. 83 (3), 321–358.

2. Lan, E.I., Liao, J.C., 2013. Microbial synthesis of n-butanol, isobutanol, and other higher alcohols from diverse resources. Bioresour. Technol. 135, 339–349.

3. Park, J.H., Lee, S.Y., 2010. Fermentative production of branched chain amino acids: a focus on metabolic engineering. Appl. Microbiol. Biotechnol. 85 (3), 491–506.

4. Bückle-Vallant, V., Krause, F.S., Messerschmidt, S., Eikmanns, B.J., 2014. Metabolic engineering of Corynebacterium glutamicum for 2-ketoisocaproate production. Appl. Microbiol. Biotechnol. 98 (1), 297–311.

5. Niu, P., Dong, X., Wang, Y., Liu, L., 2014. Enzymatic production of alpha-ketoglutaric acid from L-glutamic acid via L-glutamate oxidase. J. Biotechnol. 179, 56–62.

6. Xu, P., Qiu, J., Gao, C., Ma, C., 2008. Biotechnological routes to pyruvate production. J. Biosci. Bioeng. 105 (3), 169–175.

7. Wieschalka, S., Blombach, B., Eikmanns, B., 2012. Engineering Corynebacterium glutamicum for the production of pyruvate. Appl. Microbiol. Biotechnol. 94 (2), 449–459.

8. Zhu, Y., Eiteman, M.A., Altman, R., Altman, E., 2008. High glycolytic flux improves pyruvate production by a metabolically engineered Escherichia coli strain. Appl. Environ. Microbiol. 74 (21), 6649–6655.

9. Van Maris, A.J., Geertman, J.-M.A., Vermeulen, A., Groothuizen, M.K., Winkler, A.A., Piper, M.D., van Dijken, J.P., Pronk, J.T., 2004. Directed evolution of pyruvate decarboxylase-negative Saccharomyces cerevisiae, yielding a C2-independent, glucose-tolerant, and pyruvate-hyperproducing yeast. Appl. Environ. Microbiol. 70 (1), 159–166.

10. Qin, Y., Johnson, C., Liu, L., Chen, J., 2011. Introduction of heterogeneous NADH reoxidation pathways significantly increases pyruvate production efficiency. Korean J. Chem. Eng. 4 (28), 1078–1084.

11. Yang, S., Chen, X., Xu, N., Liu, L., Chen, J., 2014. Urea enhances cell growth and pyruvate production in Torulopsis glabrata. Biotechnol. Prog. 30 (1), 19–27.

12. Miyazaki, M., Shibue, M., Ogino, K., Nakamura, H., Maeda, H., 2001. Enzymatic synthesis of pyruvic acid from acetaldehyde and carbon dioxide. Chem. Commun. 18, 1800–1801.

13. Liu, L., Hossain, G.S., Shin, H.-D., Li, J., Du, G., Chen, J., 2013. One-step production of a-ketoglutaric acid from glutamic acid with an engineered L-amino acid deaminase from Proteus mirabilis. J. Biotechnol. 164 (1), 97–104.

14. Yang, Y., Chen, Q., Guo, J., Hu, Z. 2015. Kinetics and methane gas yields of selected C1 to C5 organic acids in anaerobic digestion. Water Res. 87: 112-8.

15. Van Lier, J.; Mahmoud, N.; Zeeman, G. 2008. 16: Anaerobic wastewater treatment. In: Biological wastewater treatment: principles, modelling and design. IWA Publishing, London, UK.

16. Müller, N.; Worm, P.; Schink, B.; Stams, A.J.M.; Plugge, C.M. 2010. Synthrophic butyrate and propinoate oxidation processes: from genomes to reaction mechanisms. Env. Microb. Reports: 2(4), 489-499.

17. Toerien, D.F.; Hattingh, W.H.J. 1969. Anaerobic digestion. I: The microbiology of anaerobic digestion. Water Research 3: 385-416.

18. Wolin, M.J. 1974. Metabolic interactions among intestinal microorganisms. Ann. J. Clin. Nutr. 27: 1320-1328.

19. Zehnder, A.J.B. 1978. Ecology of methane formation. In: Mitchell R (ed). Water Pollution Microbiology. Vol II: 349-376. John Wiley and Sons, London.

20. McInerney, M.J.; Bryant, M.P; Pfennig, N. 1979. Anaerobic bacterium that degrades fatty acids in syntrophic association with methanogens. Arch. Microbiol. 122: 129-135.

21. Stams, A.J.M.; Plugge, C.M. 2009. Electron transfer in syntrophic communities of anaerobic bacteria and archaea. Nature Reviews: Microbiology: 7, 568-577.

22. Kleerebezem, R.; Joosse, B.; Rozendal, R.; Van Loosdrecht, M.C.M. 2015. Anaerobic digestion without biogas? Rev. Envorin. Sci. Biotechnol.: 14: 787-801.

23. Lee, H-S.; Salerno, M.B.; Rittmann, B.E. 2008. Thermodynamic evaluation on H_2 production in glucose fermentation. Environ. Sci. Technol: 42, 2401-2407.

24. Lindeboom, R.E.F. 2014. Autogenerative high pressure digestion: Biogas production and upgrading in a single step. PhD thesis, Wageningen University, Wageningen, NL.

25. Prescott, L.M.; Harley, J.P.; Klein, D.A. 2002. Microbiology, 5th ed.; McGraw-Hill: New York.

26. Saint-Amans, S.; Girbal, L.; Andrade, J.; Ahrens, K.; Soucaille, P. 2001. Regulation of carbon and electron flow in Clostridium butyricum VPI 3266 grown on glucose-glycerol mixtures. J. Bacteriol.: 183 (5), 1748-1754.

27. Hungate, R.E. 1966. The rumen and its microbes. New York Academic Press, New York, NY, USA.

28. Kleerebezem, R.; Stams, A.J.M. 2000. Kinetics of syntrophic cultures: a theoretical treatise on butyrate fermentation. Biotechnol. Bioeng. 67, 529-543.

29. Schink, B. 1992. Syntrophism among prokaryotes. In: Balows A, Trüper HG, Dworkin M, Harder W, Schleifer KH, editors. New York: Springer-Verlag. Vol I, 276-299.

30. Schink, B. 1997. Energetics of syntrophic cooperation in methanogenic degradation. Microbiol. Mol. Biol. Rev. 61: 262-280.

31. Stams, A.J.M. 1994. Metabolic interactions between anaerobic bacteria in methanogenic environments. Antonie van Leeuwenhoek 66: 271-294.

32. Wallrabenstein, C.; Schink, B. 1994. Evidence of reversed electron transport in syntrophic butyrate or benzoate oxidation by Syntrophomonas wolfei and Syntrophus buswellii. Arch. Microbiol. 162: 136-142.

33. Conrad, R.; Schink, B.; Phelps, T.J. 1986. Thermodynamics of H_2-consuming and H_2-producing metabolic reactions in diverse methanogenic environments under in situ conditions. FEMS Microbiol. Ecol. 38: 353-360.

34. Ahring, B.K.; Westermann, P. 1987a. Kinetics of butyrate, acetate and hydrogen metabolism in a thermophilic, anaerobic, butyrate-degrading triculture. Appl. Environ. Microbiol 53: 434-439.

35. Ahring, B.K.; Westermann, P. 1987b. Product inhibition of butyrate metabolism by acetate and hydrogen in a thermophilic coculture. Appl. Environ. Microbiol. 54: 2393-2397.

36. Dolfing, J.; Tiedje, J.M. 1998. Acetate inhibition of methanogenic, syntrophic benzoate degradation. Appl. Environ. Microbiol. 54: 1871-1873.

37. Dong, X.; Cheng, G.; Stams, A.J.M. 1994. Butyrate degradation by Syntrophospora bryantii in coculture with different methanogens and in pure culture with pentenoate as electron acceptor. Appl. Microbiol. Biotechnol. 42: 647-652.

38. Fukuzaki, S.; Nishio, N., Shobayashi, M.; Nagai, S. 1990. Inhibition of the fermentation of propionate to methane by hydrogen, acetate and propionate. Appl. Environ. Microbiol. 56: 719-723.

39. Hoh, C.Y.; Cord-Ruwisch, R. 1996. A practical kinetic model that considers end product inhibition in anaerobic digestion processes by including the equilibrium constant. Biotechnol. Bioeng. 51: 597-604.

40. Kaspar, H.F.; Wuhrmann, K. 1978. Product inhibition in sludge digestion. Microb. Ecol. 4: 241-248.

41. Labib, F.; Ferguson, J.F.; Benjamin, M.M.; Merigh, M.; Ricker, N.L. 1993. Mathematical modeling of an anaerobic butyrate degrading consortium: predicting their response to organic overloading. Environ. Sci. Technol. 27: 2673-2683.

42. McCarty, P.L. 1982. One hundred years of anaerobic treatment. In Hughes DE, Stafford DA, Wheaty BI, Baader W, Lettinga G, Nyns EJ, Verstraete W (eds). In Anaerobic Digestion 1981: 3-22. Elsevier, Amsterdam.

43. McCarty, P.L.; Smith, D.P. 1986. Anaerobic wastewater treatment. Environ. Sci. Technol. 20: 1200-1206.

44. Powell, G.E. 1984. Equalisation of specific growth rates for syntrophic associations in batch cultures. J Chem. Technol. Biotechnol. 34B: 97-100.

45. Siegrist, H.; Renggli, D.; Gujer, W. 1993. Mathematical modeling of anaerobic mesophilic sewage sludge treatment. Wat. Sci. Technol. 27: 25-36.

46. Warikoo, V.; McInerney, M.J., Robinson, J.A.; Suflita, J.M. 1996. Interspecies acetate transfer influences the extent of anaerobic benzoate degradation by syntrophic consortia. Appl. Environ. Microbiol. 62: 26-32.

47. Yang, S.; Jianghua, L.; Hyun-dong, S.; Long, L.; Guocheng, D.; Jian, C. 2016. Biotechnological production of alpha-keto acids: current status and perspectives. Bioresource Technology 219: 716-724.

48. Kumari, A. 2018. Glycolysis. In: Sweet Biochemistry: remembering structures, cycles and pathways by mnemonics. Chapter I: 1-5.

49. Agler, M.T.; Wrenn, B.A.; Zinder, S.H.; Angenent, L.T. 2011. Waste to bioproduct conversion with undefined mixed cultures: the carboxylate platform. Trends Biotechnol. Vol. 29 (2): 51-104.

50. Angenent, L.T.; Karim, K.; Al-Dahhan, M.H.; Wrenn, B.; Domíguez-Espinosa, R. (2004). Production of bioenergy and biochemicals from industrial and agricultural wastewater. Trends Biotechnol. 22: 477-485.

51. McInerney, M.J.; Bryant, M.P. 1981. Basic principles of bioconversions in anaerobic digestion and methanogenesis. In: Sofer, SS.; Zaborsky, O.R. (eds): Biomass conversion processes for energy and fuels. Plenum Press: 277-296.

52. Yu, A.Q.; Pratomo Juwono, N.K.; Jan Leong, S.S.; Wook Chang, M. 2014. Production of fatty acid-derived valuable chemicals in synthetic microbes. Front. Bioeng. Biotechnol., Vo. 2 (78): 1-12.

53. Murali, N.; Srinivas, K.; Ahring, B.K. 2017. Biochemical production and separation of carboxylic acids for biorefinery applications. Fermentation, 3 (22): 1-25.

54. Syahirah Ramli, N.A.; Saidina Amin, N.A. 2018. Thermo-kinetic assessment of glucose decomposition to 5-hydroxymethyl furfural and levulinic acid over acidic functionalized ionic liquid. Chem. Eng. Journal, Vol. 335: 221-230.

55. Cavalcanti, P.F.; van Haandel, A.; Lettinga, G. 2002. Effect of carbon dioxide and ammonium removal on pH changes in polishing ponds. Water Sci. and Technol. 45: 377-382.

56. Deffeyes, K.S. 1965. Carbonate equilibria: a graphic and algebraic approach. Limnology and Oceanography 10: 412.

57. Zhang, X.; Tao, Y.; Wang, H.; Ghasimi, D.; Hendriks, A. Protocol for VFA analysis. Sanitary Engineering Section, TU Delft.

58. APHA Standard Methods for the examination of water and wastewater: 20th Edition. 2005. American Public Health Association/ American Water Work Association / Water Environment Federation, Washington D.C.

59. Kato, S.; Yoshida, R.; Yamaguchi, T.; Sato, T.; Yumoto, I.; Kamagata, Y. 2014. The effects of elevated CO_2 concentration on competitive interaction between aceticlastic and syntrophic methanogenesis in a model microbial consortium. Frontiers in Microbiol., Vol. 5 (575): 1-8.

60. Rittmann, B.; Banaszak, J.E.; Reed, D.T. 2002. Reduction of Np(V) and precipitation of Np(IV) by an anaerobic microbial consortium. Biodegradation 13(5): 329-342.

61. Stams, A.J.M.; Kremer, D.R.; Nicolaij, K.; Weenk, G.; Hansen, T.A. 1984. Pathway of propionate formation in Desulfobulbus propionicus. Archives of Microbiology, Vol. 139 (2-3): 167-173.

62. Lablb, F.; Ferguson, J.F.; Benjamin, M.M.; Merigh, M.; Ricker, N.L. Anaerobic butyrate degradation in a fluidized bed reactor: effects of increased concentrations of H_2 and acetate. Environ, Sci. Technol., 26: 369-376.

63. Alberty, R.A. 2003. Thermodynamics of biochemical reactions. John Wiley & Sons, Inc., Hoboken, New Jersey.

64. Flamholz, A.; Noor, E.; Bar-Even, A.; Milo, R. 2012. eQuilibrator – the biochemical thermodynamics calculator. Nucleic Acids Res. 40:D770-5.

65. Metzler, D.E.; Metzler, C.M. 1978. Biochemestry: the chemical reactions of living cells. Vol I. Academic Press Inc., U.S.

66. Infantes, D.; Gonzalez del Campo, A.; Villaseñor, J.; Fernandez, F.J. 2012. Kinetic model and study of the influence of pH, temperature and undissociated acids on acidogenic fermentation. Biochemical Engineering Journal 66: 66-72.

67. Van den Heuvel, J.C.; Beeftink, M.H.; Verschuren P.G.; de Beer, D. 1992. Determination of the critical concentration of inhibitory products in a repeated fed-batch culture. Biotechnol. Tech. 6: 33-38.

68. Terracciano, J.S.; Kashket, E.R. 1986. Intracellular conditions required for initiation of solvent production by Clostridium acetobutylicum. Appl. Environ. Microbiol. 52 (1): 86-91.

APPENDIX A - THERMODYNAMIC CALCULATIONS

A.1. Thermodynamic Calculations for the Pyruvate Experiments

Table A-1. Overview of the stoichiometries of the main catabolic reactions in the pyruvate degradation experiments

Reaction No.	Reaction Stoichiometry	$\Delta G^{\circ\prime}$ [kJ/reaction]
Fermentation/Acetogenesis		
I.	Pyruvate to Acetate $CH_3COCOO^- + H_2O \rightarrow CH_3COO^- + H_2 + CO_2$	-52.0 *
II.	Pyruvate to Acetate and Propionate $CH_3COCOO^- + \frac{1}{3} H_2O \rightarrow \frac{2}{3} CH_3COO^- + \frac{2}{3} CO_2 + \frac{1}{3} CH_3CH_2COO^-$	-75.9
IIIa.	Pyruvate to Succinate $CH_3COCOO^- + 2H_2 + CO_2 \rightarrow {}^-OOCCH_2CH_2COO^- + H_2O + H^+$	-98.4
IIIb.	Succinate to Propionate $^-OOCCH_2CH_2COO^- + H^+ \rightarrow CH_3CH_2COO^- + CO_2$	-25.3
IV.	Propionate to Acetate $CH_3CH_2COO^- + 2H_2O \rightarrow CH_3COO^- + 3H_2 + CO_2$	+71.7
Methanogenesis		
V.	Acetate to Methane $CH_3COO^- + H^+ \rightarrow CH_4 + CO_2$	-35.7

* Example calculation $\Delta G^{0'}$ for reaction I (Pyruvate to Acetate):

$$\Delta G^0 = \sum_{i=1}^{n} Y_i * G_f^0 =$$

$$\Delta G^0 = (-1 * -474.6) + (-1 * -237.18) + (1 * -369.41) + (1 * 0) + (1 * -394.36) = -52.0$$

$$\Delta G^{0\prime} = \Delta G^0 + R.T_s.\ln[(1 * 10^{-7})^{Y_H}]$$

$$\Delta \boldsymbol{G^{0\prime}} = (-52) + (8.314 * 10^{-3}).(298.15).\ln[(1 * 10^{-7})^0] = \mathbf{-52.0}$$

Table A-2. Gibbs free energy changes for the main catabolic reactions in the pyruvate degradation experiments assuming **1 Pa H_2 partial pressure**

	ΔG [kJ/reaction]				
Reaction No.	**Equilibrium pCO_2 [pH]**				
	0.2 [6.9]	**1.0 [6.6]**	**1.3 [6.5]**	**1.9 [6.4]**	**3.3 [6.2]**
Fermentation/Acetogenesis					
I. Pyruvate to Acetate	-105.1 **	-100.9	-100.3	-99.3	-97.9
II. Pyruvate to Acetate and Propionate	-92.1	-89.3	-88.9	-88.2	-87.3
IIIa. Pyruvate to Succinate	-32.2	-34.5	-34.6	-35.0	-35.3
IIIb. Succinate to Propionate	-33.9	-31.5	-31.4	-31.1	-30.8
IV. Propionate to Acetate	-48.7	-44.6	-43.9	-43.0	-41.5
Methanogenesis					
V. Acetate to Methane	-32.5	-30.1	-30.0	-29.7	-29.4

** Example calculation ΔG for reaction I (Pyruvate to Acetate), pCO_2 of 0.2 bar and pH_2 of 1 Pa (Note: metabolite concentrations are as described in Section 4.2 and presented in Table 4-4):

$$\Delta G^0 = \sum_{i=1}^{n} Y_i * G_f^0 =$$

$$\Delta G^0 = (-1 * -474.6) + (-1 * -237.18) + (1 * -369.41) + (1 * 0) + (1 * -394.36) = -52.0$$

$$\Delta G = \Delta G^0 + RT\ ln\frac{[Ace^-]^1 * [pH_2]^1 * [pCO_2]^1}{[Pyr^-]^1 * [H_2O]^1}$$

$$\Delta G = -52 + (8.314 * 10^{-3}) * 308.15 * ln\frac{[0.35 * 10^{-3}]^1 * [1 * 10^{-5}]^1 * [0.2]^1}{[12.5 * 10^{-3}]^1 * [55.39]^1}$$

$$\Delta \boldsymbol{G} = -52 + (8.314 * 10^{-3}) * 308.15 * ln\frac{[0.35*10^{-3}]^1*[1*10^{-5}]^1*[0.2]^1}{[12.5*10^{-3}]^1*[55.39]^1} = \mathbf{-105.1}$$

Table A-3. Gibbs free energy changes for the main catabolic reactions in the pyruvate degradation experiments assuming **60 Pa H_2 partial pressure**

ΔG [kJ/reaction]					
Reaction No.	**Equilibrium pCO_2 [pH]**				
	0.2 [6.9]	**1.0 [6.6]**	**1.3 [6.5]**	**1.9 [6.4]**	**3.3 [6.2]**
Fermentation/Acetogenesis					
I. Pyruvate to Acetate	-94.6	-90.4	-89.8	-88.8	-87.4
II. Pyruvate to Acetate and Propionate	-92.1	-89.3	-88.9	-88.2	-87.3
IIIa. Pyruvate to Succinate	-53.2	-55.5	-55.6	-56.0	-56.2
IIIb. Succinate to Propionate	-33.9	-31.5	-31.4	-31.1	-30.8
IV. Propionate to Acetate	-17.3	-13.1	-12.5	-11.5	-10.1
Methanogenesis					
V. Acetate to Methane	-32.5	-30.1	-30.0	-29.7	-29.4

A.2. Thermodynamic Calculations for the Butyrate Experiments

Table A-4. Overview of the stoichiometries of the main catabolic reactions in the butyrate degradation experiments

Reaction No.	Reaction Stoichiometry	$\Delta G^{\circ\prime}$ [kJ/reaction]
Fermentation/Acetogenesis		
I.	Butyrate to Acetate $CH_3CH_2CH_2COO^- + 2H_2O \rightarrow 2CH_3COO^- + H^+ + 2H_2$	+48.1
II.	Butyrate to Propionate $CH_3CH_2CH_2COO^- + 2H_2O \rightarrow CH_3CH_2COO^- + CO_2 + 3H_2$	+71.5
Methanogenesis		
III.	Hydrogen to Methane $4H_2 + CO_2 \rightarrow CH_4 + 2H_2O$	-130.7
IV.	Acetate to Methane $CH_3COO^- + H^+ \rightarrow CH_4 + CO_2$	-35.7

Table A-5. Gibbs free energy changes for the main catabolic reactions in the butyrate degradation experiments assuming **1 Pa H_2 partial pressure**

ΔG [kJ/reaction]					
Reaction No.	**Equilibrium pCO_2 [pH]**				
	0.2 [6.9]	**1.0 [6.6]**	**1.5 [6.5]**	**2.0 [6.4]**	**3.5 [6.2]**
Fermentation/Acetogenesis					
I. Butyrate to Acetate	-60.9	-59.2	-58.6	-58.0	-56.8
II. Butyrate to Propionate	-52.1	-47.9	-46.9	-46.2	-44.7
Methanogenesis					
III. Hydrogen to Methane	-3.0	-7.1	-8.1	-8.9	-10.3
IV. Acetate to Methane	-31.8	-29.4	-29.0	-28.8	-28.6

Table A-6. Gibbs free energy changes for the main catabolic reactions in the butyrate degradation experiments assuming **60 Pa H_2 partial pressure**

ΔG [kJ/reaction]					
Reaction No.	**Equilibrium pCO_2 [pH]**				
	0.2 [6.9]	**1.0 [6.6]**	**1.5 [6.5]**	**2.0 [6.4]**	**3.5 [6.2]**
Fermentation/Acetogenesis					
I. Butyrate to Acetate	-40.0	-38.2	-37.6	-37.0	-35.8
II. Butyrate to Propionate	-20.6	-16.5	-15.4	-14.7	-13.3
Methanogenesis					
III. Hydrogen to Methane	-44.9	-49.0	-50.1	-50.8	-52.3
IV. Acetate to Methane	-31.8	-29.4	-29.0	-28.8	-28.6